Australian Government
Department of Defence
Defence Science and
Technology Group

Extreme Vertical Gusts in the Atmospheric Boundary Layer

Douglas J Sherman

Aerospace Division
Defence Science and Technology Group

DST-Group-TR-3160

ABSTRACT

When an aircraft is being designed, it is necessary to know the probability distribution of extreme vertical gusts in the atmosphere so the aircraft will not be overloaded. The currently accepted probability distributions are based on a relatively small quantity of data: insufficient to adequately sample moderate or large gusts. Recently, new statistical models have been developed based on a much greater quantity of data than earier models. However, the new models appear to be much too severe in the lowest 5,000 ft of the atmosphere. This may be due to mistakenly identifying a few manoeuvre loads as gust loads. It is contended that extreme gusts in the lowest layers are only those caused by thunderstorms or mountain waves and that these are no more frequent in the lowest 5,000 ft than in the 5,000-10,000 ft layer, although milder gusts may be more frequent. This document seeks a peer review of this contention. In order to guide formal discussion, a review of all causes of significant gusts has been attempted so that the peer review can address the various single issues involved.

Published by

Aerospace Division
Defence Science and Technology Group
506 Lorimer St
Fishermans Bend, Victoria 3207 Australia

Telephone: 1300 333 362
Fax: (03) 9626 7999

AR-016-419
July 2015

APPROVED FOR PUBLIC RELEASE

Extreme Vertical Gusts in the Atmospheric Boundary Layer

Executive Summary

This paper contains a critical review of the gust statistics required for the design, testing or certification of aircraft. A mission analysis type of gust clearance requires a probability distribution of extreme gusts. A new statistical model of gust probability has recently been developed based on far more data than was available previously. However, when the new distribution was used in an attempt to provide a gust clearance for a transport aircraft, the numbers of severe gusts predicted at low altitudes was severely over-estimated in comparison to in-service experience.

The classical gust model embodied in U.S. Military Standards and the Federal Aviation Regulations was based on a relatively small quantity of data: sufficient to define the probability of occurrence of mild gusts, but insufficient to accurately define the probability of moderate or severe gusts which are much less frequent.

There have been a number of programs in recent years that have collected large quantities of normal acceleration data from various aircraft, but attempts to automatically distinguish manoeuvres from turbulence have not always been satisfactory. This is particularly significant in the lowest altitude band of the atmosphere because this is where civil transport aircraft perform most of their manoeuvres. During initial climb and final descent, airspeeds are usually low. Aircraft are very insensitive to gusts at low speed, so any manoeuvre that was misinterpreted as a gust would imply a very large gust magnitude. A very few such misinterpretations would have a significant effect on the statistics of the rare, extreme gusts.

In the lowest 5,000 ft, boundary layer effects make small to moderate vertical gusts very frequent. If extrapolated to large values, this would suggest that large gusts are also very frequent. But the writer considers that the only processes that could cause severe gusts are thunderstorms and mountain waves. These phenomena seem unlikely to intensify towards the ground: if anything vertical gusts would be lessened by ground proximity. It might be expected that these phenomena will have the same frequency in the lowest 5,000 ft as in the next 5,000 ft. If this hypothesis can be justified, then separate calculations show that the resultant gust model produces much more realistic predictions of aircraft experience of extreme turbulence.

This report reviews possible causes of significant gusts in the lowest 5000 ft and seeks a peer review of the probability of encountering severe gusts at low altitude. A corrected statistical model of gust intensity is essential for future aircraft gust clearance or certification through mission analysis methods.

Author

Douglas J Sherman
Aerospace Division

Dr Sherman has worked for over 40 years at DST Group, or its forebears, on the determination of the various forces that act on an aircraft, especially those due to atmospheric turbulence. He is currently an honorary fellow at DST Group.

Contents

.

List of Definitions

Adiabatic Lapse Rate	The rate of change of temperature with altitude that would occur if a parcel of air was transported sufficiently rapidly to each altitude to prevent loss or gain of heat.
Continuous Turbulence method	A method of aircraft design which is also known as the Power Spectral method (*q.v.*).
Discrete Gust method	A method of aircraft design that requires the structure to survive a gust of a specific shape, magnitude and duration specified in the applicable design code. Because typical aircraft flexibility has changed since the introduction of this method, it has now been superseded by the Tuned Discrete Gust method (*q.v.*).
Equivalent Air Speed (EAS)	An adjusted value, U_e, of the true air speed, U_T, that has the same momentum flux at sea level air density as the true air speed has at altitude.
Gust Model	An abbreviation for a statistical model of gust probability
Inversion	A layer in the atmosphere where the potential temperature increases with height.
Limit Load	The greatest load that an aircraft is expected to experience in its lifetime. An aircraft must be able to support limit load without detrimental permanent deformation. (See also "Ultimate Load".)
Mission	A description of a typical flight type, by breaking it into segments with a given duration, altitude, speed, weight and aircraft configuration for each segment.
Mission Analysis	A typical set of missions is analysed to find the probability of encountering a gust, load or strain of any given magnitude.
Monin-Obukhov Length	This is a scale length (usually denominated L) that is used to non-dimensionalise velocity profiles in the Atmospheric Boundary Layer, particularly in the lower tenth of the boundary layer (the Surface Layer). The concept is too complex to consider thoroughly here. A physical interpretation is that, during the day, $-L$ is the height at which the buoyant production of turbulence kinetic energy is equal to that produced by the shearing action of the wind. The theoretical formula involves cross-correlations that are only measured in experimental programs. [See, for example, Chapter 10 of Wyngaard (2010).] For practical application, L can be estimated from normally recorded variables by methods such as that described by Hess and Spillane (1988).

Potential Temperature	The potential temperature is the temperature that a parcel of air would have if it were brought adiabatically to 1000 hectopascal (hPa), i.e. with no loss or gain of heat as the parcel was moved. (This simple definition only holds if no condensation or evaporation of water occurs in the hypothetical movement.)
Power Spectral method	A method of aircraft design in which the turbulence is modelled as a Gaussian random variable with a prescribed power spectral shape. This method assumes the aircraft responds linearly to gusts of different magnitude or shape. It allows for aircraft flexibility, so was an improvement on the earlier Discrete Gust method. However, the advent of non-linear responses in aircraft systems (notably gust alleviation) has made this method unsuitable for large modern aircraft. In these cases it is usually considered to be superseded by some form of the Tuned Discrete Gust method.
Statistical Discrete Gust method	A method of aircraft design in which the shape of the design gust is varied as a succession of rises and falls with various durations and at various time delays. The shape of the rises and falls is selected from a particular family of shapes. The design gust magnitude varies with the number of rises or falls. The method is currently considered too computer intensive for normal design use but has been tested experimentally.
Super-adiabatic Layer	A layer where the potential temperature at the bottom of the layer is warmer than the potential temperature at the top of the layer.
True Air Speed (TAS)	Actual distance travelled divided by time taken.
Tuned Discrete Gust method	A method of aircraft design in which the input gust is of prescribed shape (almost invariably 1 period of a 1-cosine shape) but the wavelength is variable. Designers have to check for a range of possible wavelengths to determine the worst response, using a full model of the aircraft including both elastic and non-linear effects. The gust magnitude varies with the wavelength: almost always the design gust magnitude is taken to be proportional to the 1/6 power[1] of the wavelength being considered.
Ultimate Load	An "ultimate load" is required to be at least 1.5 times the magnitude of limit load. An aircraft is required to withstand an ultimate load for at least three seconds without failure. If an applied load is greater than ultimate load or if ultimate load is maintained for more than 3 seconds, a major structural failure, such as a broken wing, is likely to result.

[1] Note: Kolmogorov (1941) turbulence scaling would predict a 1/3 power, but experimental measurements of the most extreme gusts indicate a smaller power. This accords with some fractal theories of turbulence.

Acronyms

ABL	Atmospheric Boundary Layer
EAS	Equivalent Air Speed
FAA	Federal Aviation Authority (U.S.)
FAR25	Federal Aviation Regulations Part 25
FCL	Free Convection Layer
LHRP	Load History Recording Program
ML	Mixed-Layer
SL	Surface Layer
TAS	True Air Speed

This page is intentionally blank

1. Introduction

This work is concerned with the gust statistics used for the design and certification of aircraft. It was triggered by recent gust certification activities in support of the Royal Australian Air Force's C-130J-30 Hercules fleet. Those certification activities used a new gust probability distribution based on a much greater database of flight records than has been used previously. However, there was a large discrepancy between the analytical prediction of the frequency of occurrence of limit load and the observed "in-service" experience.

The statistical model of gust probability (hereafter shortened to "gust model") used in current codes such as the various U.S. military specifications and the U.S. Federal Aviation Regulations Part 25 (FAR25) was based on some 8,700 hours of flight data (Hoblit et al. 1966). This was sufficient to estimate probabilities of mild gusts, but not of moderate or severe gusts. More recently, de Jonge (1994) has proposed a gust model based on some 2 million hours of flight data, but this model has not received much use because it has not been recognised by the regulation authorities. Even with 2 million flight hours, the probability of the most extreme gust velocities has required extrapolation from the number of occurrences of lesser gust magnitudes.

Careful consideration of the C-130J-30 certification activities has led to the contention that the recently developed gust statistics are unrealistically severe at low altitudes. This is thought to be because, outside of specific meteorological phenomena (thunder storms, mountain waves and possibly dust devils), there are no mechanisms in the lowest part of the atmosphere which would produce such extreme gusts.

The intent of this paper is to promote discussion within the meteorological and aeronautical research communities as to whether this contention is correct. To facilitate communication between the communities, this paper will keep explanations simple and minimise the mathematics involved.

2. Background

2.1 Aircraft Certification

To certify the safety of an aircraft it is required to demonstrate that:

- Gusts large enough to damage the aircraft will only occur with an acceptably low frequency,
- Metal fatigue due to the occurrence of smaller, but frequently repeated, gusts will not cause premature failure[2] of an aircraft,
- For supersonic aircraft, that "unstarting" of the flow through the engines due to a gust will only occur at an acceptably rare interval.

[2] Design for fatigue is a discipline in itself that will not be elaborated in this paper.

For all these purposes, it is necessary to have reliable statistics of the frequency of occurrence of gusts of various magnitudes.

2.2 Gust Statistics

The gust component that most affects an aircraft is the component, *U*, perpendicular to both the wing and the flight path. In normal horizontal flight, this is the vertical component of the gust velocity.

The traditional statistics used for power spectral[3] gust load design of civil aircraft have been defined in Appendix G of the Federal Aviation Regulations (FAR) (1980). The statistics used for the design of military aircraft Garrison (1971) have a different form, but are essentially identical save for some special requirements for very low altitude flying.

These statistics were chosen by (Hoblit et al. 1966) who based his statistical model on the data that had been collated by Neuls et al. (1962). Table 1 indicates the size of the database on which several statistical models of gust frequency were based. Hoblit's model, developed for the Federal Aviation Authority (FAA), is denoted here as the "Classical Power Spectral" model.

Table 1: Database sizes for principal gust model codes and other studies

Code	*Year*	*Flight Hours*	*Flight Miles*
NACA TN 4332	1958	Unknown	Unknown
Classical Power Spectral	1962	8,700	2,373,067
ESDU 69023	1969	33,000	6,541,400
Lockheed LHRP[4]	1986	(?) 1,059,990	(?) 159,000,000
de Jonge et al	1994	2,000,000	1,600,000,000

Most power spectral models of gust frequency, including the FAA model, specify that *N(U)*, the rate of exceedance of a gust magnitude *U*, has the form:

$$N(U) = N_0 \left[P_1 \times exp\left(\frac{-|U|}{b_1}\right) + P_2 \times exp\left(\frac{-|U|}{b_2}\right) \right] \qquad 1.$$

Here, N_0 is the rate of exceeding the mean value of the gust[5]. The parameters P_1, P_2, b_1, b_2 vary with altitude and are specified in FAR25[6]. Using the FAR25 parameters, equation 1 may be graphed as shown in Figure 1.

[3] The two most used methods of gust load design are designated the "Discrete Gust" method and the "Power Spectral Gust" method.
[4] Load History Recording Program
[5] The mean value of vertical gust is generally assumed to be zero–hence the subscript 0–but the same formula is also applied to stresses and other load quantities that may have a finite mean value.

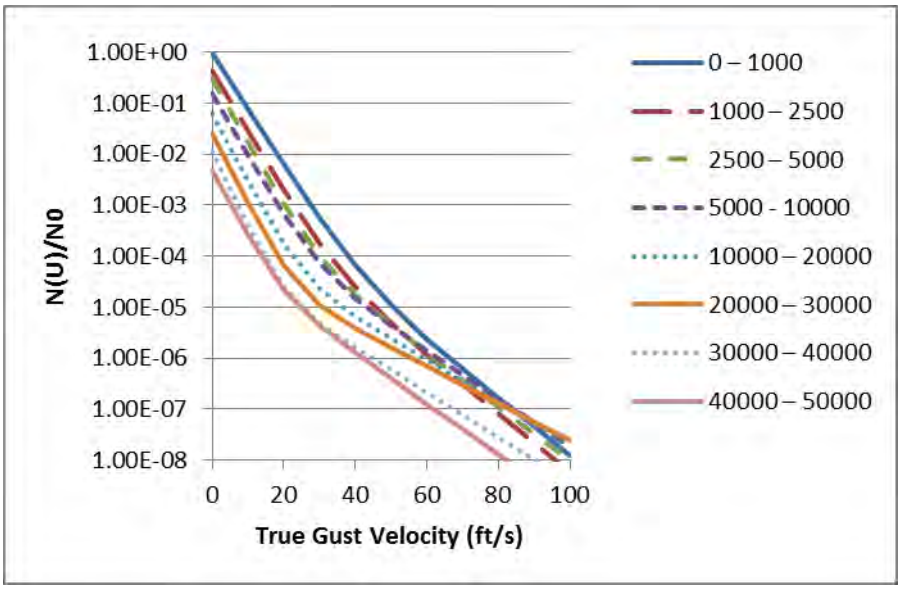

Figure 1: Probability of exceeding a true gust velocity at various altitudes (ft) using FAR statistics

The important thing to note from equation 1 and Figure 1 is that gust magnitudes are assumed to be unbounded: they just become less probable as the gust magnitude increases. Physically it might be expected that gust magnitudes must be bounded at some level, even when occurring in such an extreme condition as a tornado. More particularly, it is desired to show that, at low altitudes, extreme gusts (i.e. those that may cause structural overload) only occur in thunderstorms and mountain waves: gusts due to all other causes are bounded at a relatively low magnitude[7].

In Figure 1, the ordinate shows, in non-dimensional form, the rate at which a given "true" gust velocity, U, is exceeded. The non-dimensionalising factor, N_0, is aircraft dependent but of the order of 1 Hz. N_0 may be calculated from the aircraft transfer function but the details are not needed for this discussion.) A typical limit load design value is 85 ft/s, though this value may vary with altitude and flight condition.

The term "true" gust velocity, (denoted U_T when clarification is required) indicates that this quantity is truly the vertical distance the air travels per unit time. Why would one use any other measure of vertical velocity? Because, using the True Air Speed (TAS) measure, a given gust at sea level will carry more momentum than at altitude, so there is a larger effect on the aircraft at sea level. This is due to the variation of air density. Just as

[6] At one time an attempt was made to explain the form of this equation as the sum of very frequent, mild gusts, occurring outside thunderstorms (the term incorporating P_1), plus very infrequent severe gusts, occurring in thunderstorms (the term incorporating P_2). That physical interpretation has now been abandoned as severe turbulence has also been found away from thunderstorms. However, the terms "non-storm" and "storm" turbulence still linger in the literature.

[7] The writer considered just posing this question but concluded that it would be better to structure the answers by making a broad survey of the main gust generating mechanisms within the ABL and so facilitate the consideration of individual phenomena.

meteorologists use "potential temperature" to eliminate the effect of atmospheric rarity at altitude, the aeronautical engineer uses "equivalent sea level velocity" to account for the same thing. The Equivalent Air Speed (EAS), U_e, corresponding to a TAS of U_T, is defined by:

$$\rho {U_T}^2 = \rho_0 {U_e}^2 \qquad 2.$$

where ρ is the air density at altitude and ρ_0 is the air density at standard sea level conditions.

2.3 Aircraft Response

The effect that a gust has on an aircraft will depend on how long the gust is maintained. In the "discrete gust" method[8] of aircraft design, an aircraft is designed to withstand a vertical equivalent gust of 50 ft/s with a 1-cosine shape and a horizontal length of 25 mean aerodynamic chords of an aircraft. (See Figure 2.) This is the gust length to which rigid aircraft have been found to respond most strongly. Aircraft will also respond to gusts which are longer or shorter but, for a given magnitude of gust, the response of the aircraft will be less.

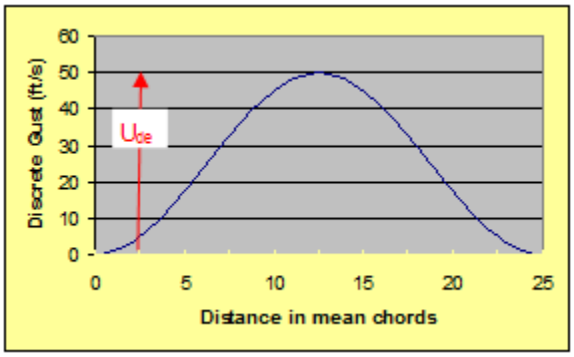

Figure 2: Shape of discrete gust used as an aircraft design criterion

The mean[9] chord of an aircraft is the average distance between leading and trailing edges of the wing. It is usually in the range between 1 m and 10 m, so the gusts under consideration have a width of between 25 m and 250 m. The rising portion of the gust is half the total gust length, so the "rise distance" is between 12.5 m and 125 m. A 50 ft/s gust[10], as an equivalent air speed, is regarded as a "limit load" condition (see the list of

[8] There are two common methods of aircraft gust design. The power spectral method is specified in terms of true gust velocity and the discrete gust method which is specified in equivalent gust velocity.

[9] The aerodynamic mean chord is a weighted mean chord but aerodynamic and geometric mean chord are, in practice, usually fairly close to each other.

[10] The difference between the 50 ft/s limit for a discrete gust analysis and the typically 85 ft/s limit for the power spectral method is due to the fact that the former method assumes all the energy is concentrated at the wavelength that most affects the aircraft, whilst the latter method assumes the disturbance energy is distributed over a complete spectrum of wavelengths.

definitions at the front of this document) because design of older aircraft (typically 1950's vintage) to this criterion has been found to be satisfactory[11].

Only a few research aircraft are equipped to directly measure the vertical component of gust velocity. In most cases, the measure of vertical gust is derived from the measured acceleration of the aircraft normal to the flight path, plus knowledge of the aircraft's airspeed, altitude, weight and other characteristics. This measure of the gust is called the "derived equivalent" gust velocity (U_{de}); the 50 ft/s magnitude is an equivalent, not a true, gust velocity.

Other hazards may occur in response to sudden changes in *horizontal* velocity. These may cause upsets to the control of the aircraft. The horizontally divergent flow in a thunderstorm downburst is an example of this possibility. The result may be just as fatal, but in this report, the main consideration is vertical gusts giving rise to structural overload[12].

Gust loads are often referred to as "turbulence", but the extreme design criterion will occur as an encounter with an organised flow structure such as a plume, a wave, a dust devil, or, in worst case, a tornado (Roach and Findlater 1983).

2.4 Effects of Gust Shape

Wingrove and Bach (1994) postulated that the organised flow structures that cause most severe aircraft gust encounters are either an updraft or a vortex. (See Figure 3.)

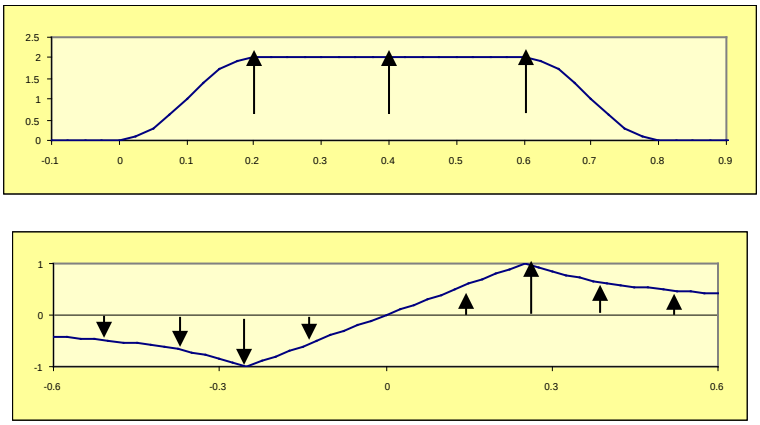

Figure 3: The two flow structures postulated to most directly affect aircraft. For present purposes the axis labels are arbitrary. Only the shape is significant.

[11] Many modern aircraft are larger and more flexible than in earlier years, so changes in the detail of structural analysis are required. However, the 50 ft/s equivalent air speed is in the right ball park for atmospheric studies.

[12] Vertical gusts sufficient to attain ultimate load may also occur in a downburst. Fujita (1986) in his Figure 4.1 shows vertical wind changing from 5 m/s upwards to almost 20 m/s downwards in a distance of about 125 m.

Jones (2004) developed the "Statistical Discrete Gust" (SDG) method of analysing an aircraft structure. This method involved a search for the waveform that maximised a selected response of an aircraft structure. This method was deemed too computer intensive for practical use at this stage, but during the evaluation phase, Hull (1994) performed a SDG analysis on a swept wing business jet. The critical input wave form for wing root vertical bending moment can be seen in Figure 4. This can be interpreted as an initial, long wavelength, negative gust that excites a rigid body mode of the aircraft. This mode continues with a positive rebound which coincides with a positive, short wavelength, gust increment exciting a dynamic mode of the wing.

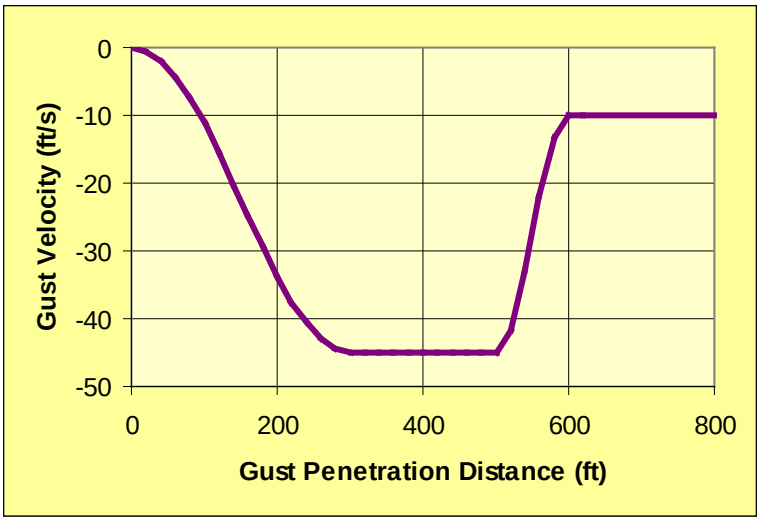

Figure 4: Critical Gust Profile for Wing Root Bending Moment of a swept wing business jet

In all the flow structures shown in Figure 3 and Figure 4, there is a change in vertical velocity over a defined distance. The effect of multiple gusts at various time delays is also important, but within the scope of what can conveniently be analysed from measured gusts, the significant output would be the change in vertical velocity as a function of the gust duration. The mean squared value of this function is, of course, the structure function of the gust velocity time series but, in, this application, it is necessary to consider extreme values rather than the mean.

3. Improved Gust Statistics

As previously indicated, the coefficients in the FAR were based on a relatively small quantity of flight data, about 8,700 flight hours (Hoblit et al. 1966), (Neuls et al. 1962). In recent years several attempts have been made to develop an improved gust model, though still using the same formula. For example, de Jonge et al (1994) (see Figure 5) who derived their model from records of about 2 million flight hours.

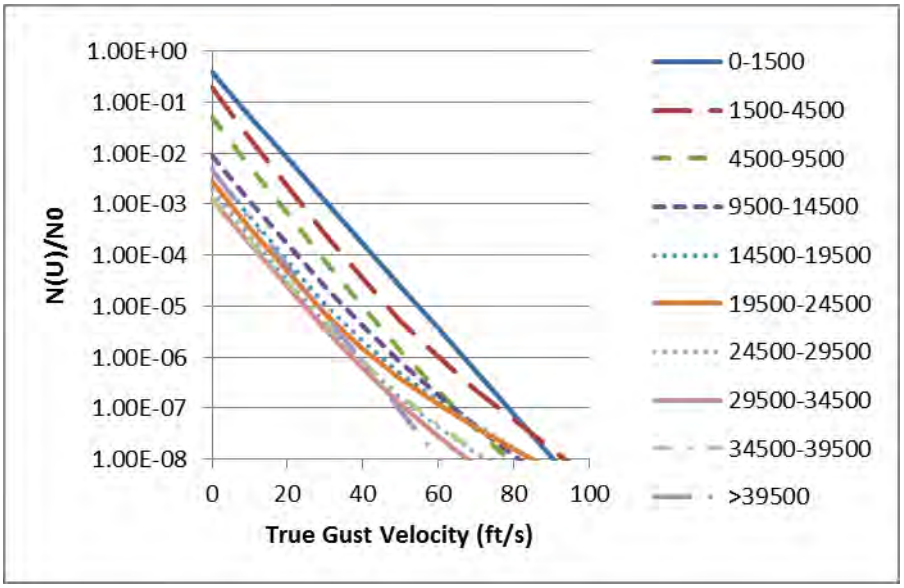

Figure 5: Probability of exceeding a true gust velocity at various altitudes (ft) using de Jonge's statistics

For low magnitude gusts, the revised statistics match fairly closely to the FAR gust model. This is to be expected because the small sample used to establish the FAR model was, nevertheless, large enough to have included a sufficient number of small gusts. This is shown in Figure 6 Because of the low air density at altitude, the effect on an aircraft is better indicated by the derived equivalent gust[13] than the true gust. See Figure 7.

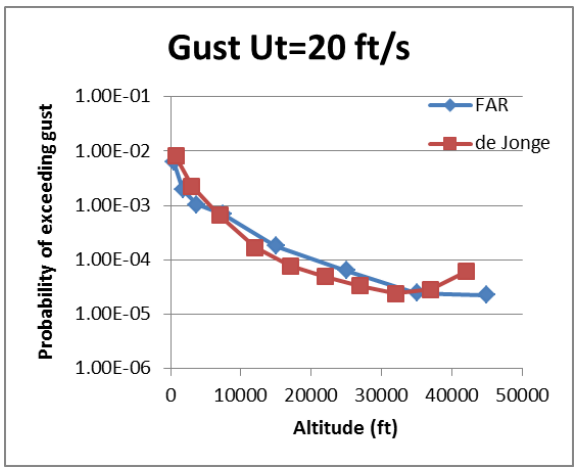

Figure 6: Probability of exceeding a mild gust with true gust velocity of 20 ft/s.

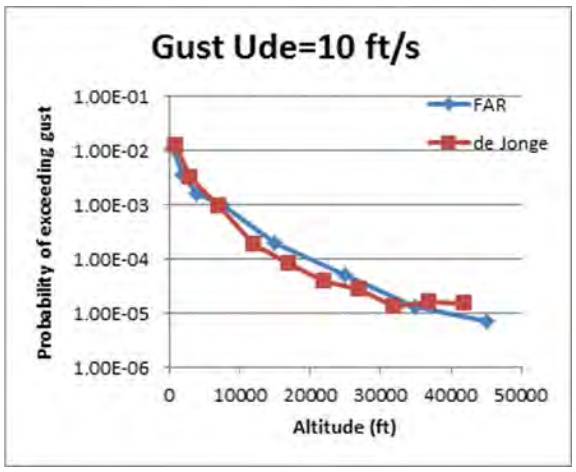

Figure 7: Probability of exceeding a mild gust with derived equivalent velocity of 10 ft/s.

[13] In this, and the following figures, the probability of exceeding a given gust is given as $N(U)/N_0$. The value of true gust velocity, U, corresponding to a given value of U_{de} is determined by the method given by Press and Steiner (1958) using their equation 18. $U_T = (\bar{C}/\bar{A}) \times U_{de}$. The values of the U_{de} multiplier are taken as those given in Press and Steiner's Table I(b) for "storm" turbulence, since this discussion is primarily concerned with gusts of large amplitude.

For a moderate gust, the difference between the two gust models is quite apparent. At the lowest altitude the revised gust model predicts more gusts than did the FAR model. However, at all altitudes above about 5,000 ft, the revised model predicts significantly fewer gusts than the FAR model. It may be seen in Figure 8 and Figure 9 that, apart from an odd value at an altitude of 37,500 ft, the curve is smooth. This indicates regularity between altitudes, which would be expected if the rate of exceedances is reliably estimated.

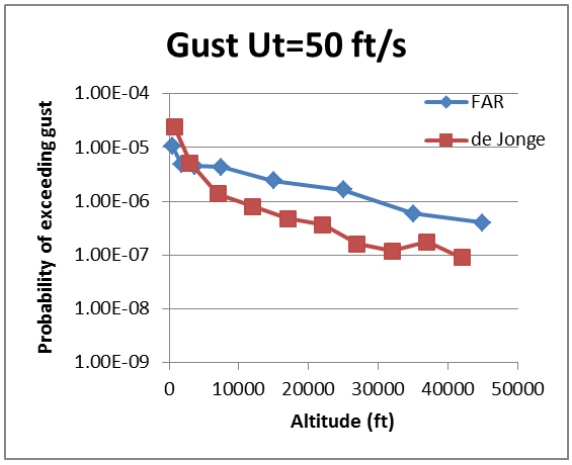

Figure 8: Probability of exceeding a moderate gust with true gust velocity of 50 ft/s.

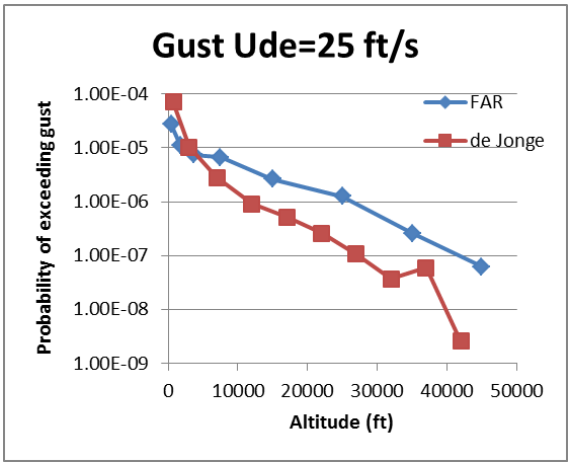

Figure 9: Probability of exceeding a moderate gust; derived equivalent gust velocity of 25 ft/s.

When the same comparison is done for a severe gust, the revised gust model shows a very irregular variation with altitude, indicating that there was insufficient data to develop an accurate model of severe gusts.

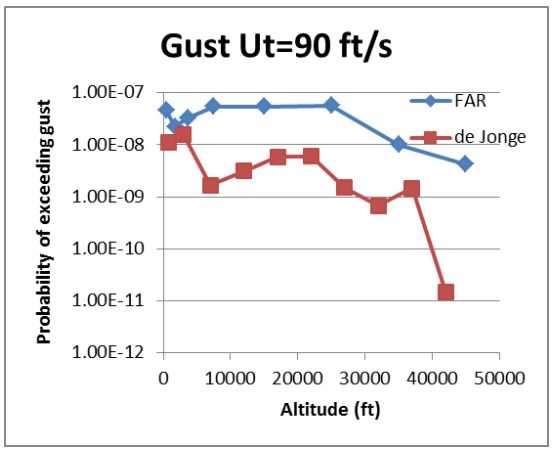

Figure 10: Probability of exceeding a severe gust with true gust velocity of 90 ft/s.

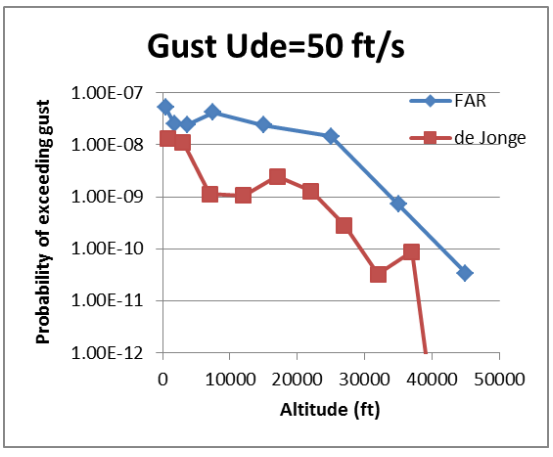

Figure 11: Probability of exceeding a severe gust; derived equivalent gust velocity of 50 ft/s.

In this discussion it has been noted that a regular variation of gust exceedances with altitude indicates reliability of the model. This may prompt the observation that the FAR25 gust model has fairly smooth curves, despite being based on a small amount of

data. In this case, the reason for the smooth curves is that smooth variations with altitude were built into the method of determining coefficients adopted by Neuls et al (1962) (see their figures 12, 13[14] and 14) and indeed, before them, by Press and Steiner (1958). However de Jonge determined all his coefficients independent of the coefficients for adjacent altitudes. Thus a smooth variation with altitude in de Jonge's model can be regarded as an indicator of reliability.

To put these gust magnitudes in context, for an aircraft cruising at a true airspeed of 200 knots and an altitude of 10,000 ft, a 10 ft/sec (EAS) gust would be expected 7 times per hour, a 25 ft/sec gust would be expected about once every 50 hours and a 50 ft/sec gust might be expected every 50,000 hours.

The main concern of the present report is the very severe gusts. The probability of exceeding a derived equivalent gust of 50 ft/s is shown in Figure 11. It is apparent that the older, FAR, code is too severe at all altitudes. But the noteworthy feature of the graph based on de Jonge et al's data is the order of magnitude rise in gust probability for flight below 5,000 ft. This result would not be surprising for mild gusts, caused by dry convection, but is not expected for severe gusts that, well below jet stream altitudes, are only expected to occur in thunderstorms or mountain waves. The probability of encountering either of those phenomena in the lowest 5,000 ft is not expected to be any greater than in the 5,000 to 10,000 ft altitude band, since both phenomena generally affect a large part of the troposphere. Moreover, to the extent that ground proximity affects either phenomenon, it will be to cause a reduction in the magnitude of the vertical gust because vertical motions will be supressed by the presence of the ground surface..

A possible reason for the apparently high probability of severe gusts in the lowest 5,000 ft altitude band derives from the fact that gust magnitudes are inferred from aircraft normal acceleration. When flying at low altitude an aircraft is likely to be doing many manoeuvring turns as it departs from, or approaches, an airport. At the same time, it is flying very slowly, which is a condition where it is very insensitive to gusts. Thus a given manoeuvre acceleration, if mis-interpreted as a gust, would suggest a very high gust velocity. It would appear, therefore, that at low altitudes, the measured probability of a severe gust may be dominated by a few accelerations resulting from aircraft manoeuvres but wrongly identified as gusts.

When de Jonge did his analysis, he had three sets of data available to him and, for each altitude band, he tried to assess which data set(s) were most trustworthy. One of these sets (in fact the largest set) came from the British Civil Aviation's CAADRP[15] program which recorded data from a large set of British Airways aircraft. To make the size of the data set manageable, the data system only recorded events when the change from 1g flight exceeded 0.5 g at some time during the event. This data set was subjected to manual identification and removal of manoeuvres from the flight record. De Jonge discounted this

[14] As seen in their Figure 13, Neuls et al (1962) fitted smooth curves of relative severity, k_1 and k_2 (hence b_1 and b_2) with altitude. This eliminated random scatter, but did not do much to overcome the errors due to the very small quantity of exceedance data for extreme gusts.

[15] Civil Aircraft Airworthiness Data Recording Program

set because, "data in the altitude range below 4,500 ft appears improbably light compared to the other two data sources". In fact, it is probably the other two data sets that should have been discounted, because one had no manoeuvre removal and the only manoeuvre removal applied to the other was an automated process to correct the normal acceleration by an increment based on the bank angle. Only a few errors in this process would make a very significant change to the deduced probability of the rare, extreme gusts.

The "mission analysis" method of design requires that the expected time between occurrences of "limit load" (see the list of definitions at the front of this document) should be at least 50,000 hours (Hoblit et al. 1966). However, a recent attempt to clear a transport aircraft using revised gust statistics (Sherman 2013) has resulted in predicted times between occurrence of limit load gusts as short as 3,000 hours if the aircraft is flying for a large proportion of time at low altitudes. Yet the aircraft has been in satisfactory use for many years, so it appears that the revised gust statistics are overly conservative. The inference is that whilst mild gusts are very frequent at low altitudes, severe gusts are exceedingly infrequent and may possibly not occur at all unless in association with thunderstorms or mountain waves. If the analysis is repeated with the rare gust statistics truncated as suggested above, the average time between limit load exceedances would be ten times longer, which is much more believable.

Lest this conclusion be wrong, this paper is a request that meteorologists consider whether there are any phenomena in the lower atmosphere, other than thunderstorms or mountain waves, which might cause severe gusts. An exhaustive list of possible sources of atmospheric gusts is examined in some detail in the following sections.

4. The Lower Atmosphere

4.1 The Atmospheric Boundary Layer

Low altitude flight occurs mainly in the Atmospheric Boundary Layer[16] (ABL), which is turbulent for much of the time. The ABL is conventionally assumed to have a thickness of the order of 1 km (~3,000 ft), though it can shrink to 200 m at night and increase to 3 or 4 km over desert if the solar radiation is intense. Thus any flight records at low altitude will contain a high proportion of turbulence. At any altitude, limit loads are encountered very rarely in normal flight, so the analysis of flight data has generally required extrapolation of the small pool of available data to obtain the probability of very severe gusts. Thus there is little actual evidence from flight data of very severe gusts in the ABL. Most of the time, the ABL is not saturated with moisture, so convection is not releasing latent heat. Thus turbulence generation mechanisms do not involve the large concentrations of energy which are seen in thunderstorms: it is possible that the gust magnitudes outside of thunderstorms and mountain waves are bounded at a fairly low value—less than the usual limit load gust.

[16] Sometimes known as the Planetary Boundary Layer.

Mountain waves and strong moist convection (often leading to thunderstorms) both affect the ABL but also affect higher altitudes to a similar extent. The probability of these phenomena resulting in severe gusts within the ABL can be extrapolated from statistics obtained at higher altitudes[17]. They will therefore be excluded from any further consideration in this paper except when specifically mentioned.

Question 1: Is there any effect of terrain proximity on mountain waves (e.g. katabatic winds) that would make the probability of associated (large) vertical gusts at low altitude significantly greater than would be predicted by extrapolation from higher altitudes?

Density currents include phenomena such as cold fronts or sea breeze fronts. These are not specifically ABL phenomena, but occur in the same altitude range, so will be included in the present survey. Thunderstorm downbursts and their associated gust fronts will be excluded because of their association with thunderstorms, but in any case, they are much more likely to cause large horizontal velocity divergence giving rise to aircraft control problems than vertical gusts of magnitude sufficient to cause direct overload of an aircraft.

The next section of this report is primarily to give some meteorological context for aeronautical engineers. The various states of the ABL will be considered, and the organised flow structures that may occur in each will be mentioned.

Following that, the rest of the document is a survey of the various low altitude flow phenomena and a discussion of the possible magnitudes of the vertical gusts that may occur in each.

4.2 States of the Atmospheric Boundary Layer

There are some significant differences between the ABL over land and over the ocean. This section will mainly be confined to the ABL over land.

The ABL is always capped by an inversion which is a stable layer. Thus it is always possible for waves to propagate at the top of the ABL. Because the density differences in air are very much less than those at a water surface, the wave amplitudes may be hundreds of times greater than the waves observed on the ocean.

Other mechanisms of gust generation depend on the state of the ABL. Several states are recognised (Stull 1988).

4.2.1 The stable boundary layer.

This usually occurs at night. Normally, the stable boundary layer is very thin, typically 200 m or less. Radiative cooling of the ground is transmitted to the air, so the lowest layers are coldest, hence densest. The stable air suppresses most turbulence and convective mixing,

[17] The proximity of the ground may act to limit vertical velocities, but this means that an extrapolation from higher altitudes is conservative, whereas de Jonge (1994) is suggesting that there are many more severe gusts than would be predicted by extrapolation.

so there is little friction to retard the air flow at higher levels in, or above, the boundary layer. Commonly a maximum in the wind speed profile occurs in the upper part of the boundary layer: this is called a low level jet, although the maximum may be only a little faster than the air flow at higher altitudes (Ulden and Wieringa 1996).

Because the air is stable, turbulence tends to be weak and intermittent, and often occurs at multiple layers. There are few mechanisms to generate large gusts other than surface roughness elements, waves or secondary flows (e.g. gravity currents generated by local terrain variations). Because the whole boundary layer is stable, waves can be internal to the ABL, not just at the inversion which occurs at the top of the layer in other states of the ABL. For reviews of some turbulence causing mechanisms that can occur in the stable ABL see Poulos et al (2002) and Sun et al (2004).

4.2.2 The unstable boundary layer.

This occurs when the ground is warmed, usually by solar radiation. In the first instance, a thin layer of air adjacent to the ground is warmed by molecular heat transfer, and this heat is then communicated to the rest of the ABL. The convective ABL is usually considered to consist of the following layers (Stull 1988):

1. The micro-layer, which has a thickness of the order of 1 cm.
   In the micro-layer, molecular processes dominate. Molecular conduction of heat, viscous transport of momentum and molecular diffusion of passive tracers are responsible for the transport in the lowest few millimetres of the atmosphere.
   Because heat transfer across this layer is by conduction rather than convection, the temperature decrease across the micro-layer is very large with temperature gradients of the order of 10^4 °C m^{-1}.
   The micro-layer is mainly recognised in the Marine Boundary Layer because the roughness of most terrestrial surfaces would disrupt it. However, over a few terrain surfaces—desert sand or rock may be one example—the roughness is small enough to permit formation of the micro-layer.
   This layer is too thin to affect aircraft, but will be significant in the later discussion of the effective temperature driving intense dry convection.
2. The Surface Layer (SL), which has a thickness of the order of 10–100 m.
   This is typically 10% of the boundary layer thickness. In the SL, large scale thermal convection is constrained by proximity to the lower boundary and heat transport is by small scale turbulent eddies. Mixing is by forced convection and appears to be explained by Monin-Obukhov similarity scaling. (See the list of definitions at the front of this report.) Turbulent fluxes are constant with height to within 20% throughout the layer.
   In the SL, the temperature gradient is unstable (super-adiabatic) and of the order of 10^{-2} to 10^{-1} °C m^{-1}.

3. The Free convection Layer (FCL) which is a transition or overlap between the SL and the Mixed Layer. This typically covers the height range from about twice the Monin-Obukhov scale length to 20% of the boundary layer thickness.
4. The Mixed Layer (ML), which usually occupies most of the boundary layer thickness.
   This is typically 80% of the boundary layer thickness. In the ML, mixing is dominated by large scale, convectively driven thermal plumes and mixing by free convection appears to follow mixed-layer similarity scaling.
   In the ML, mixing is very effective, so the change of potential temperature with height is small and the wind speed is close to uniform.
5. The Entrainment Zone or Interfacial Layer (IL). This is the top of the ABL and can be very variable in height. Wyngaard (2010), on p. 193, says that the IL can have a thickness as much as 20 – 50% of the mean depth of the boundary layer, though perhaps 10% is more common. [Fairall et al(1997)]
   In the IL, intermittent turbulence, overshooting thermals, Kelvin-Helmholtz waves, internal waves, and sometimes clouds may be found.

The general structure of the flow in the convective boundary layer has been described by Hess et al (1988) on the basis of field measurements by Webb (1977), (1984). Figure 12, shows the pattern of the flow. The boundary layer thickness is denoted by the symbol h. In the lowest part of the surface layer, there are very strong gradients of both potential temperature and wind speed. In the mixed layer, these parameters are nearly constant.

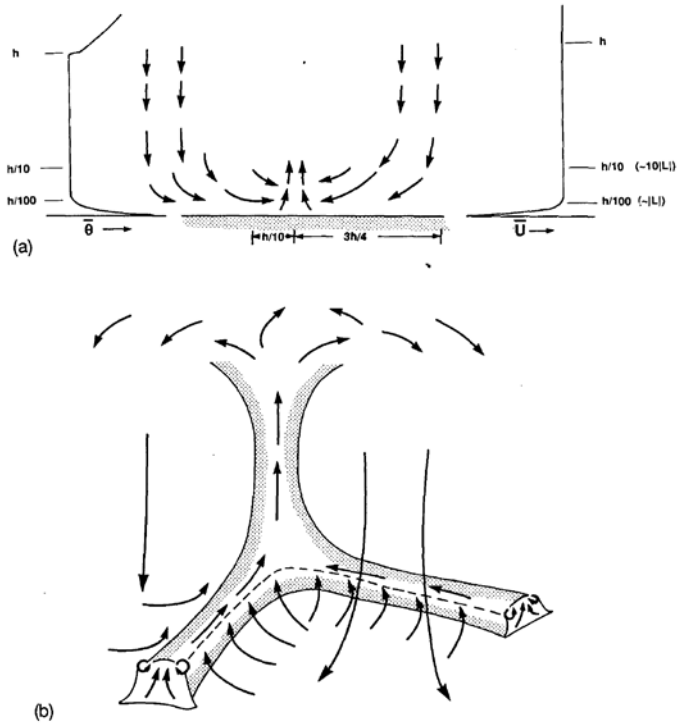

Figure 12: Flow pattern in a strongly convective atmospheric boundary layer [after Hess et al (1988)] The upper figure is a side elevation, whilst the lower is an isometric projection.

In plan view, the surface flow is divided up into irregular hexagonal cells. At the nodes where three cell boundaries meet, there is a thermal, rising up to the top of the boundary layer. Surrounding each thermal there is a return downflow that divides into three descending cores. Where these cores strike the ground, approximately in the centre of the three hexagonal cells surrounding the thermal, the flow diverges and sweeps the hot air adjacent to the ground towards one or other of the cell walls. These walls are about $0.1h$ wide and $0.1h$ high. The hot air in these walls tends to rise, but the walls also act as conduits to channel the hot air more or less horizontally, to the base of the thermal.

4.2.3 The neutral boundary layer.

This may occur when an unstable boundary layer loses its input radiative energy. This typically occurs towards the end of the day, and the resultant deep neutrally-stratified layer extends into the night with the new stable boundary layer growing below it. It may also occur when cloud overcasts the sky. Mixing may continue for a short time, until the layer is homogenised to a uniform potential temperature.

In these conditions, convective turbulence decays but mechanical turbulence may continue, caused by the wind shear between the free atmosphere above the boundary layer and the ground below. Few other mechanisms that cause organised flow structures giving rise to gusts are known, although it may be that weak turbulence can sometimes be generated by upward-propagating gravity waves (forced by flow over low-relief terrain),

the presence of critical layers caused by wind turning with height, and shear in the upper part of the low-level jet. [See (Tjernström et al. 2009); (Conangla and Cuxart 2006)].
The next section will survey the gust causing processes in the altitude band associated with the ABL. It is important to note how the ABL differs from the boundary layers encountered in the engineering context. The Earth's rotation is important and the temperature structure is as important as the variation of horizontal velocity throughout the layer.

5. Mechanisms that Generate Gusts

Consider each of the mechanisms that may generate gusts of sufficient magnitude to affect an aircraft. It is desired to quantify the maximum gust that may be produced by each mechanism. In aiming to establish such bounds, there is some similarity with the analysis of Graf et al (2010) who considered bounds on potential temperature in a convective boundary layer.

5.1 Turbulence

Gusts strong enough to cause a limit load will usually occur in organised flow structures. However, it is conceivable that ABL turbulence may contain large eddies that occasionally cohere sufficiently to cause a significant aircraft load.

Turbulence has the appearance of a random process, within which gust velocities have an approximately normal probability distribution. Gusts sufficiently strong to cause a limit load are extremely rare: much rarer than the conventional "two or three standard deviations". It is these extreme values that deviate most from a normal probability distribution. Sorbjan (1989) states, on page 206, that, "Homogeneous turbulence is observed to be Gaussian, and departure from Gaussian behaviour is associated with inhomogeneity." It is questionable whether a truly homogeneous flow can ever be realised in the atmosphere. Dutton et al (1968) showed that gust velocities measured by aircraft were slightly non-Gaussian, with the most significant discrepancy occurring with the strongest gusts. For gusts greater than three standard deviations, the probability of occurrence progressively rose above that of a Gaussian process, with the strongest gusts being several orders of magnitude more probable than with a Gaussian distribution. Therefore it would not be safe to predict severe gust probabilities on the basis of a Gaussian model.

Kaimal et al (1976) show that the length scale of the horizontal wind components remains fairly constant with altitude throughout the ABL but the length scale of the vertical component increases rapidly with altitude, especially in the lowest 10% of the ABL. It is conventional to assume that the length scale for the vertical component is equal to the altitude up to an altitude of about 2,500 ft. Since aircraft require a length scale to be at least 25 to 250 m, significant gusts due to turbulence are only likely to occur above the surface layer. But, above the SL, wind shear is much weaker than at lower altitudes so it may be expected that convective structures will dominate over wind shear. But these convective

structures have organisation due to physical reasons: they are unlikely to be chance eddies occuring in phase.

The previous paragraph is a purely heuristic argument, but it suggests that any large gust in the ABL is much more likely to be in a convective structure than in the conjunction of random turbulent eddies. Random turbulence may, therefore, be ignored as a cause of large gusts.

5.2 Plumes and Thermals

In the Surface Layer (SL), plumes of relatively warm air are relatively small in diameter, typically 100 m across, and correspondingly close together. Because there is a velocity gradient in the SL, the plumes tend to lean forward in the direction of travel, and travel faster than the surface wind. Williams and Hacker (1992), (1993) (subsequently abbreviated to WH92 and WH93) indicate that the plumes tend to merge as they rise in the SL. It is unclear to what extent surface layer plumes are swept into the convective cell "walls".

As mentioned previously, there is a transition zone between the SL and the ML called the Free Convection Layer (FCL). In this layer, the multiple small plumes feed into larger thermal columns of rising air that are typically 1 km across and continue ascending through the ML to the top of the boundary layer. These rising thermals are surrounded by a field of downdrafts. Because the wind tends to be uniform with height in the ML, the thermals tend to be vertical.

Experimental, airborne, measurements of these structures have been reported in WH92 and WH93 who use the terms "surface layer plumes" and "mixed layer thermals" for the two structures. Williams and Hacker suggest that with a typical wind profile, the mixed layer thermals will move faster than the surface layer plumes, so the particular plumes that feed into a given thermal will vary with time.

Williams and Hacker also review the evidence for roughly hexagonal patterns of "walls" between points where downdrafts descend to the surface. Hot surface air is swept to these walls by the diverging downdrafts, and it then flows to wall intersections which are usually the base of a mixed layer thermal. [See Figure 12.] This pattern of flow concentrates the flow to the base of the thermal into three relatively thick channels (the "walls") and so reduces the friction that would be involved in a uniform shallow radial inflow to the base of the plume. It may also help to explain some observed dust devil behaviour.

From the time series and composite plots in WH92 (Figs 2-5) and WH93 (Figs 4, 5, 7-13), together with the velocity scales (w_* and u_*) listed in WH92 Table 1, it may be deduced that changes in vertical velocity across mixed layer thermals (~0.5-2 km across) can reach and occasionally exceed 5-6 m/s, whilst across surface layer plumes (100-200m across) they can reach and occasionally exceed 4-5 m/s. This agrees generally with Stull (1988) who, on page 444, stated that the average vertical velocity in a SL plume was 1 m/s with fluctuations of the order of 5 m/s, whilst on page 461 he stated that vertical velocities in

ML thermals can reach 5 m/s or more, although weaker updrafts of 1 to 2 m/s are more common.

Since the vertical velocities in plumes and thermals are so far below a 15 m/s (50 ft/s) design gust, it seems unlikely that dry convection in non-rotating thermal flows will ever be a concern in regard to aircraft limit load.

5.2.1 Dust Devils

Under certain conditions, some plumes develop a rotating character as a vortex with an approximately vertical axis. If there is sufficient dust in the air, these rotating plumes may be seen as dust devils (known as willy willies or whirly whirlies in Australia). It is possible that the stabilising effect of the rotation may permit the dust devil to develop greater vertical velocities than in a SL plume.

Ryan and Carroll (1970) measured the horizontal and vertical wind speed at 2 metre altitude by moving a wheeled tower into the path of a number of dust devils. They obtained data from about 80 encounters, and developed an equation for w_{max}, the maximum vertical wind component at 2 m altitude:

$$w_{max} = A_1 (g h_3)^{1/2} \left(\frac{\gamma_3}{\gamma_d}\right) \left(\frac{z_{2m}}{L}\right)^{1/2} \qquad 3.$$

where A_1 is a dimensionless constant, g is the acceleration due to gravity, h_3 is the thickness of the (mildly super-adiabatic) ML (typically several hundred metres), γ_3 is the lapse rate in the ML (typically 1.1 to 1.8 °C per 100 m), γ_d is the dry adiabatic lapse rate, z_{2m} is 2 metre and L is the Monin-Obukhov scale height. The greatest value of w_{max} that they observed was 7.2 km/h (2 m/s or 6.6 ft/s).

In contrast, on page 109 of his thesis, Sinclair (1966) states, "On either side of the dust devil centre, (r=0) in all cases and at all levels, the vertical velocity usually reaches 10 m/s and then falls off toward zero rather rapidly as r is increased. In addition, the regions of maximum vertical motion tend to expand radially from the lower to the upper level[18]."

The reason for the large discrepancy between the observations of Sinclair and of Ryan and Carroll is not known. Stull, on page 448, states that once the tangential velocity is sufficient to pick up dust from the ground, a vertical velocity of around 4 m/s is required to carry fine dust aloft. Perhaps this suggests that the site where Ryan and Carroll made their measurements had unusually fine dust or very low density dust, so that very mild dust devils could be identified.

Stull states that dust devil depths of 100 m are typical. This may suggest that vertical velocities decrease to less than 4 m/s by about 100 m altitude. It is possible, however, that at greater altitudes, the vertical velocity may increase again as suggested below.

[18] The lower level was at 7 ft and the upper level at 31 ft.

It is necessary to consider how the vertical velocity in a dust devil varies as altitude increases to levels where aircraft fly. Sinclair (1966) produced a composite figure (see Figure 13) based on 14 sailplane penetrations of the upper airflow associated with low-level dust devils.

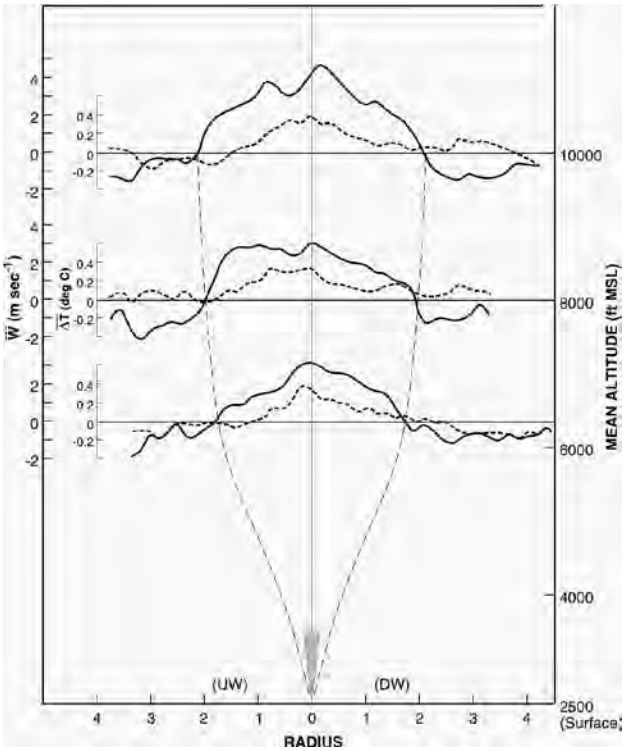

Figure 13: Vertical velocity in plumes in which dust devils are embedded. [After Sinclair (1966)]

Figure 13 gives some idea of how upper level vertical gust velocities vary with altitude in the updraft thermals in which the dust devils are embedded. As intimated two paragraphs previously, Figure 13 suggests that, following a decrease in vertical velocity near the top of the surface layer, the vertical velocity may increase again with height in the mixed layer.

Bell (1967) reported on a pilot balloon ascent near a dust devil. The normal rate of rise of the balloon was 310 m per minute. The actual rate of rise could be inferred from the altitude at successive 1 minute intervals as shown in Table 2. In this table, the "corrected" data is the vertical velocity of the air once the balloons normal rise (310 m/minute) has been subtracted. The peak value of 610 m/minute (approximately 10 m/s) is about two thirds of the typical discrete gust design value, although Figure 13 shows that this gust might be spread out over a rather larger distance than 12.5 mean aerodynamic chords. Table 2 bears out the suggestion in Figure 13 that the vertical velocity increases with height in the upper part of the mixed layer. In this case, the maximum vertical velocity at the top of the ML is about 10 m/s.

Table 2: Vertical velocities observed by a pilot balloon ascending near a dust devil (after Bell, 1969)

Minutes	Height (m)	Difference per minute	
		Raw	Corrected
1	600	--	
2	1200	600	290
3	1820	620	310
4	2700	880	570
5	3620	920	610
6	3990	370	60
7	4300	310	0
8	4610	310	0

Typical vertical extents of around 100 m (Stull 1988) would suggest that dust devils may be related to surface layer plumes. However, their rotating nature may make them behave in a special manner. For example, whereas non-rotating surface layer plumes tend to merge with each other as they rise, the rotating plumes may preserve their identity. The fact that Sinclair was able to detect dust devils at upper levels in the mixed layer supports this possibility.

However, to state a typical height of a visible dust devil as 100 m is an over-simplification. Hess and Spillane (1990) noted that the visible dust clouds in dust devils tend to have two preferred heights: either 9% of the boundary layer height or 51% of the boundary layer height. They relate these two heights to different parts of an inferred structure of convective flow. The taller dust devils are thought to form at the vertex of intersecting lines of up-draft convergence (i.e. inside ML thermals), whilst the shorter dust devils are limited by the height of the "walls" or channels which transport the hot air to the base of the thermal (see Figure 12). Similarly, Cantor, Kanak et al (2006) in their paragraph 80, report that a Martian dust devil appears to have a height of 0.57 times the inferred planetary boundary layer depth and Ansmann et al (2009) show, in their figure 2, vigorous plumes rising to around 2 km in a dust layer that is about 4 km thick. As seen in Figure 13, Sinclair shows that the plumes extend right up to the top of the boundary layer.

It appears, however, that dust devils become much milder near the top of the surface layer, since they are no longer visible, so must be unable to suspend dust. This is an important observation for aircraft flying at these heights. One wonders what physical phenomenon might cause the swirling updraft to slow down to the point that it can no longer suspend the visible dust. A likely possibility is the entrainment of ambient air, which reduces the temperature difference that drives them to rise from the ground, though another possibility is the breakdown of a swirling vortex with the formation of a bubble of reversed flow on the vortex axis. [See Lopez (1990) and Brown and Lopez (1990).] Note that Kaimal and Businger (1970) observed a downdraft embedded at the centre of a dust devil.

Where dust devil thermals extend high in the ABL, the lack of dust means that there is no evidence whether dust devils continue to rotate. Williams and Hacker (1992) (see their fig 12) note a slow clockwise turning of thermals on average in the middle of the ML, which

they note could be due to averaging a few strongly rotating thermals with a larger number of non-rotating thermals.

5.2.2 Modelling Updrafts in Deep Convection and Dust Devils

The most severe forms of convection occur in tropical cyclones, thunderstorms, tornadoes and dust devils.

- The first three of these involve moist convection with major energy release from latent heat, released as water vapour condenses in rising updrafts. Many moist updrafts extend right through the troposphere until they reach the tropopause, which is a very stable layer. Convection is particularly deep in tropical regions, where the Hadley cell combines with the thermal updrafts to produce extremely deep thunderstorms and an extremely high tropopause. The most severe updrafts overshoot into the lower parts of the stratosphere before falling back, resulting in entrainment of stratospheric air into the troposphere and growing the height of the tropopause.
- Dry plumes, thermals and dust devils only involve sensible heat, so they have a lower energy supply. They are bounded by the inversion at the top of the ABL but, again, vigorously rising updrafts will overshoot and entrain air from above the ABL, resulting in a growing boundary layer thickness. Typically the ABL has a thickness of around a kilometre but, over fiercely heated deserts, the intense dry convection that causes dust devils can grow the boundary layer to heights of as much as 4 km [see e.g. Ansmann et al (2009)].

Renno and Ingersoll (1996) have considered a portion of the atmosphere as a heat engine in order to develop upper bounds on the magnitudes of updrafts. They identify a section of the atmosphere that can be considered as approximately self-contained in regard to its heat cycle. For example, they consider a rising thunderstorm plume together with its surrounding field of descending air. Appendix A: contains an analysis that follows Renno in considering maximum updrafts in both thunderstorms and in dust devils. Under worst possible conditions, as shown in Table 5 in that appendix, the extreme updraft in a thunderstorm is predicted to be between 24 and 53 m/s and in a dust devil between 14 and 32 m/s, depending on the value assumed for one of the coefficients in Renno's equation. As indicated previously in this paper, thunderstorms are known to contain the potential to cause a structural overload to an aircraft, but thunderstorm avoidance techniques are well known and practiced. The thunderstorm analysis does, however, provide a useful reality check on the application of Renno's equation.

Renno's equation is based on the assumption that the atmosphere performs as a heat engine with maximum possible efficiency. i.e. the heat cycle is reversible. Renno realises that no physically achievable process is truly reversible. To the extent that the atmospheric heat engine is not a reversible process, the extreme values given in Table 5 in the appendix will be an over-estimate. It is uncertain as to how much of an over-estimate.

As a separate issue, the meaning of the vertical velocity computed by Renno's equation needs to be distinguished from the vertical gust velocity used for aircraft design. Renno calls w the "convective velocity", which is the updraft within the rising plume / thermal. As this is computed on an energy basis, it is expected to be a maximum updraft velocity. In comparison, the aircraft design gust velocity is really the change in vertical velocity that an aircraft encounters in a horizontal distance of 12.5 chords (12.5 m to 125 m). If the rate of change of the convective velocity at the edge of the plume / thermal is small, an aircraft will adjust to the different velocity with no significant load caused to the aircraft. However, if the plume / thermal edge has a width of the order of 100 m, then the gradient is a real concern.

Question 2: What is known about the rate of change of vertical velocity with radial distance at the side of a plume? What is the range of thickness of the shear layer at the side of a plume[19]?

The lateral extent of a dust devil is very much smaller than that of a thunderstorm. The dust generally marks the strong updraft portion of the dust devil. The transition to this maximum value is in the clear air around the core. Since the larger dust cores are typically 10 to 100 m diameter, it is likely that the transition distance will also be of this general magnitude, and so tune with the maximum response of an aircraft. The worst case modelling, using Renno's method as in the appendix, predicts a vertical velocity of 14 to 32 m/s, although, to the best of the writer's knowledge, such a large velocity has not been measured in a dust devil. 14 m/s is very little below the gust limit load design case of 50 ft/s (15 m/s). It may be possible for meteorologists to develop operational forecasts of parameters in Renno's equation (e.g. solar insolation[20] and depth of convective layer) and, using these, to produce forecasts of maximum dust devil gusts. There appears to be a real possibility that damaging gusts may occur in dust devils under worst conditions.

The rotation of a dust devil will give it a longer life and greater stability. It is still unknown what causes a small proportion of convective plumes or thermals to rotate. In the case of the tall dust devils that extend well through the mixing layer, it may be that as the mean flow moves a thermal forward, the walls or channels that feed hot air to its base may lag behind. If one of those channels is aligned predominantly perpendicular to the direction of travel of the thermal, the flow in it may have a significant moment of momentum about the axis of the thermal and so set it in rotation[21]. This leaves the question of the shorter dust devils that only extend through the depth of the surface layer. Perhaps surface layer plumes have an as yet unrecognised similarity to mixed layer thermals, in that they, too, have small channels or walls feeding hot air to their base.

---

[19] Edges of SL plumes and dust devils can be sharp (plumes have a micro-front at the leading edge; dust devils are strengthened by their vortex): so max w change can be up to 5 m/s in 100m.
Edges of ML thermals, however, are rarely sharp or even well-defined, due to lateral detrainment (Stull 1988 pp464-466; see also Crum et al. 1987, J. Clim. Appl. Meteorol. 26, 774-788).

[20] The work of Eissa et al. (2013) may be useful in developing a forecasting tool for solar insolation.

[21] It would be interesting to run Kathy Kanak's CFD model of intense dry convection and impose occasional puffs of wind at upper levels to see if they triggered thermals into rotation.

Question 3: Further consideration needs to be given to the generation of dust devils when the cause of the intense updrafts is a cold air outflow over a relatively warm surface. Are there any factors acting (e.g. suddenness of the cold flow) that might make the problem different from the archetypal gradually increasing heat over a desert.

5.3 Density Currents

Sea breezes, thunderstorm outflows and cold fronts are all physically similar, but differ in size[22]. They cause lift as the cold air advances underneath the ambient air. [See Simpson (1969) and Charba (1974).]

5.3.1 The Density Current Head: Vortex Generation

In the head of an advancing front more or less vertical clefts have been shown to exist (Simpson 1969). It has been hypothesised that these are preferred sites for the formation of vertical axis vortices. [See Cowled (1988) and Simpson (1969).] Similar clefts in cold outflows from thunderstorms have been linked with tornadogenesis [Mueller and Carbone (1987), Wilson (1986) and McCaul and Bluestein (1986)], although tornadoes are part of the hazard of thunderstorms, so will not be further considered here[23]. Dry vortices at the leading edge of a cold outflow are discussed in the observation at the end of the above analysis of dust devils (which includes the "invisible dust devils" that occur when dust is not available to mark the swirling updraft).

Question 4: What is the mechanism and quantitative analysis for generation of vertical axis vortices at the leading edge of a cold front?

5.3.2 The Density Current Head: Uplift

The remaining phenomenon to consider is the updraft forced by the advancing cold front of a density current as it wedges underneath the warmer air. Thunderstorm outflows may be severe because large amounts of moisture can lead to extreme amounts of evaporative cooling. Since they are, again, associated with thunderstorms, they will, for the most part, be ignored as a possible cause of gusts that exceed an aircraft limit load. However, they are part of a continuum of similar phenomena, so will be included in the discussion as a phenomenon that may inform the consideration of sea breezes and other density currents. Moreover, some thunderstorm outflows run far ahead of their parent storm and may even continue after the storm has ended. In these cases, the uplift is distinct from that induced

[22] As a consequence of the greater size of cold fronts and, to a lesser extent, sea breezes (Clarke 1983) Coriolis forces affect the horizontal flow to a greater extent than with thunderstorm outflows. However, the generation of vertical velocities by the intrusion of a dense low level layer is much the same.

[23] Admittedly, tornadoes probably affect the lowest 5,000 ft more than the 5,000-10,000 ft altitude band; though not much is known of what altitude tornadic circulations persist to inside a thunderstorm cloud. On the other hand, tornadoes are most visible in the lowest layers (below the cloud) and would be avoided by all means possible. The writer has not found any reports of tornado encounters below cloud level, though a near approach by a helicopter was described by Tyrell (1999).

by moist convection associated with a thunderstorm. The typical example of this type of outflow is the "haboob[24]" which was first identified in Africa and Saudi Arabia. Membery (1985) has described two notable examples of this phenomenon.

Simpson (1969), reviewed the knowledge about gust fronts. He cited theoretical work by Defant (1921) who calculated the flow around an elliptical body as shown in Figure 14.

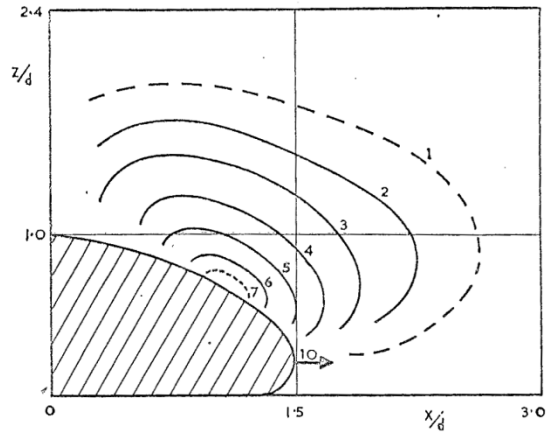

Figure 14: Potential flow updrafts at nose of density current simulated as an elliptical body [After Simpson (1969)]

His analysis showed updrafts at the head of a front of up to 7 units when the gust front was advancing at a speed of 10 units. This model was an idealisation in that the front was assumed to be a rigid surface, with no flow across it. Whilst this seems intuitive, it will be seen shortly that aircraft measurements sometimes appear to show a different picture. Simpson pointed to order of magnitude support for Defant's gust magnitudes in glider measurements of updrafts up to 2 m/s for a front advancing at 2.5 m/s (radar measurement) against a headwind of about 1.5 m/s.

Subsequent work by Finkele et al (1995) used aircraft measurements to show that the region of updraft at the head of a sea breeze front is much smaller than is predicted by Defant's model. Figure 15 and Figure 16 show the flow around the sea breeze head at two successive times. The front was defined by the region of increased moisture content. At both times there was a small region of updraft, just ahead of the front, at about 30% of the head's maximum height. There were also vertical currents ahead of the front at about 80% of the head's maximum height but whilst, at the earlier time, these were updrafts, at the later time they were downdrafts. These figures also show the off-shore "return current" at around 1000 m altitude. See the note about this in Appendix B: .

[24] A haboob is a dust storm raised by the gust front outflow from a thunderstorm. Named from the Arab word "hbb" meaning "to blow".

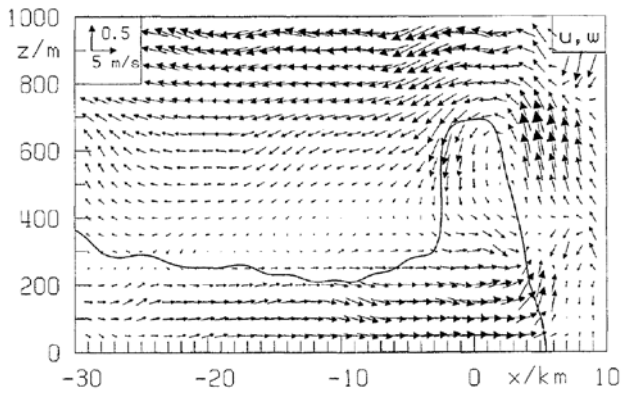

Figure 15: Flow around sea breeze head at 11:19 Local Solar Time (LST). The coast is at x = 0. [After Finkele et al (1995)]

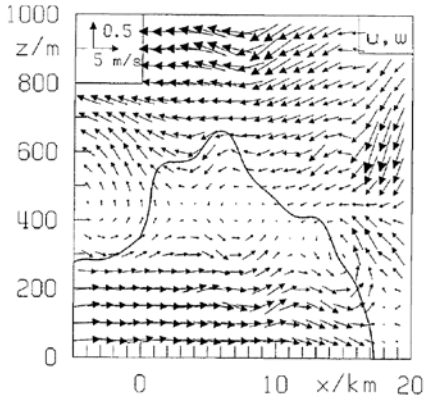

Figure 16: As for the previous figure, but at 13:06 LST. [After Finkele et al (1995)]

At the earlier time, the potential temperature dropped from 20°C before the front to 16.5°C behind the front, and at the later time, from 22°C ahead of the front to 17.5°C at the rear. The temperature drops were 3.5°C and 4.5°C respectively. The speed of advance of the front was about 12 km in 107 minutes or 1.9 m/s.

Simpson (1969), using reported observations, showed a relationship between speed of advance of a density current and the temperature drop across the front. Simpson fitted a curve with the square of the frontal speed varying in proportion to the temperature drop. A frontal advance speed of 14 m/s corresponded to a temperature drop of 10°C[25]. Finkele et al's speed of 1.9 m/s is a little low for a temperature drop of 4°C, but not unduly so given the scatter in Simpson's graph. The maximum updraft in front of the head was around 0.5 m/s, which is about 25% of the speed of advance of the front. This is much less than the 70% predicted by Defant.

What is unexpected about the flow pattern reported by Finkele et al. is that there is a flow through the front of the humid air. This suggests that the real front is ahead of the humid air, with the sea breeze containing dryer air at its forward edge. This air may have been entrained from the environmental air into which the sea breeze is intruding.

Such entrainment of large masses of environmental air may possibly be understood in terms of the three dimensional structure of a gust front. This has been studied, using laboratory models, by Simpson (1969) (see Figure 17). In plan view, an advancing front is a convoluted surface, with convex bulges reaching forward ahead of the general line of the front. In the real atmosphere, the shape of a gust front can be visible when it carries dust, as in the case of a haboob. Idso (1976) describes it thus:

[25] Apart from thunderstorm related incidents, the greatest temperature drops plotted by Simpson were measured in African gust front dust storms (haboobs).

> "The leading edge of a haboob is always changing its appearance. According to T.J. Lawson of the University of Reading, who has studied haboobs in the Sudan, 'A push of cold air from within the body of the haboob will cause the formation of a bulge or lobe, which appears to grow forward at a slightly faster rate than the average speed of the front. The lobe will expand vertically and horizontally until, when its forward movement relative to the front has decreased, irregularities will start to appear in its leading edge, causing any fresh surge of air moving up from behind to flow to one side. In this way new lobes are continually appearing out of the dying stages of a previous one.'".

Idso continues:

> "I have often seen two adjacent lobes expand simultaneously and engulf a large volume of intervening warm air. Expanding cold lobes also overrun a certain amount of the warmer air in front of them."

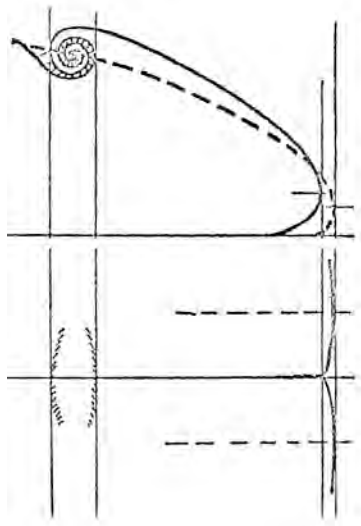

Figure 17: Gust front vertical cross-sections and (below) plan view of convoluted front. The solid line in cross-section is located on the solid line in plan view, whilst the dashed line cross-section corresponds to the dashed line in plan view. (After Simpson, 1969)

Thus, the gust front, including the entrained air, possibly extends forward to the limit of the domains shown in Figure 15 and Figure 16. Finkele et al note that, despite filtering to remove small fluctuations in the vector field, the air ahead of the gust fronts contains convection cells, for which reason they only showed a very limited forward extent in their vector plots. Wood et al (1999) show similar cross-sections of a sea breeze measured by an instrumented aircraft but use a slightly different definition of the front of the sea breeze. Wood et al show convective plumes just ahead of the front, which make it impossible to separately distinguish the vertical gust field caused by the intruding sea breeze. The best that may be attempted is to note that the gust front speed of advance was 1.25 m/s, the temperature drop across the gust front was around 4°C and the vertical gusts in the convection ahead of the front reached updrafts of 4 m/s. This gust front speed is even lower than that measured by Finkele et al for the same temperature drop, so is rather low in comparison with Simpson's relationship.

Sea breezes are very mild examples of density currents. A more extreme case is found in one of the haboobs described by Membery (1985), He noted an unusually fast haboob travelling at 40 kn. (20 m/s) which would suggest a peak upgust of around 14 m/s on the basis of Defant's 70% model, or 5 m/s on the basis of Finkele et al's 25% model.

Arritt (1993) has determined the peak vertical velocity in the whole domain around a numerically simulated sea breeze front. Unfortunately, due to limitations of the then available computers, he was constrained to use a horizontal grid spacing of 5 km, which resulted in a very low average vertical velocity of 0.9 m/s.

At an extremely simplistic level, the vertical velocity generation may be considered to be due to the displacement of warm air by the under-running cold air. Suppose a density current head of height H and length L travels at speed U. The time for the head to pass a point is *L/U*. Assuming a triangular shape head, the volume of fluid displaced by a unit width of gust front is *½ H L*. The average induced vertical velocity is volume displaced divided by (length of head x time). Thus the average vertical velocity is *½ (H/L) U*. Now the length of the head is typically twice the height, so this gives the vertical velocity of *0.25U*, in accord with Finkele et al's observations. A typical head is usually shaped somewhere between triangular and rectangular, so the typical induced vertical velocity would be between *0.25U* and *0.5U*.

5.3.3 Cold Fronts

It is uncertain whether cold fronts, themselves, act as density currents or whether they are simply preferred sites for triggering moist convection which results in evaporatively driven outflows. The process of frontogenesis is the process of creating or steepening the temperature gradient of a front. During this process the atmosphere reacts in an attempt to restore balance, the consequence is a circular motion along the front where air is being lifted up, along the cold front and dropping downward, behind the frontal boundary. So there is an updraft at the front of a cold front, even if the forward advance of the front is related to dynamic processes rather than being gravity driven.

The commonly studied northern hemisphere cold fronts usually occur in moist air, so the updrafts tend to trigger moist convection which increases the updraft through release of latent heat. Many of these cases will develop into thunderstorms, so can be ignored for the purposes of this paper. It is not known how often cold fronts may trigger moist convection of low vertical extent, which does not lead to thunderstorms.

Reeder and Smith (1992) have reviewed the knowledge of cold fronts and especially as it applies to the Southern hemisphere. Terrain, latitude, surface heating and moisture supply all have major effects on their behaviour. The cold air mass that moves in behind a cold front may be very thick, but Reeder and Smith show examples of Australian cold fronts where the leading edge was very thin and the cold air only reached a thickness of 1 km after 150 km of air had passed over the observer. Krause et al (2000) explain this, "In Southern Australia summertime deep cold fronts are frequently preceded by a shallow cold frontal line connected to a prefrontal lower tropospheric trough. The advance of this line defines a "cool change" which in many cases causes severe weather events."

Kraus et al have described an aircraft encounter with a notable vortex embedded in the head of a density current within such a shallow cold frontal line. The vertical velocity changed from -12 m/s to + 10 m/s in a flight distance of approximately 900 m. This change is considerably more than the 15 m/s (50 ft/s) limit load specified in the FAR. However, the ramp length over which the change occurred is much more than 12.5 chord lengths of the biggest current regular passenger transport aircraft. The occurrence is certainly notable: the question to be investigated is how close this is to the worst case that occurs in a density current head. The altitude was low, approximately 500 m above sea level, so differences between true air speed and equivalent air speed will not be significant.

Question 5: Is there data on maximum vertical gusts occurring in conjunction with dry cold fronts and with moist cold fronts that do not develop into thunderstorms?

Question 6: Are there any histograms of temperature drops behind sea breezes, cold fronts and haboobs? Are there any other forms of density currents that should be considered?

5.4 Waves in the ABL

5.4.1 Katabatic Flows

There is an overlap of phenomena between mountain waves and density currents because density currents in the form of katabatic flows occur when cold dense air flows down sloping terrain. Well known examples, often associated with mountain waves, are the (European) Foehn wind and the (North American) Chinook wind. In Australia there has been some investigation of the Adelaide "Gully Wind". Such flows can travel at supercritical speeds down the slope and transition to sub-critical flow through an hydraulic jump (Grace and Holton 1990) with its associated large scale eddies. There is a need to consider whether the hydraulic jump can cause sufficient gradient of vertical wind component to cause an aircraft overload.

5.4.2 Mountain Waves

Mountain lee waves are known to sometimes cause gusts greater than an aircraft can withstand. Since these have been well recognised as a hazard to aircraft, they will not be further considered. However, a distinction will be drawn between "mountain lee waves" and other waves formed on stable layers on or within the ABL.

5.4.3 Stable Layers

The capping inversion on the ABL is a stable layer. Within the ABL there may be other inversions, as when a sea breeze with a lower depth than the ABL may have flowed inland. A nocturnal boundary layer may be stable throughout its whole depth, so it may be regarded as an inversion of thickness equal to that of the entire boundary layer. And, in the morning, above a growing boundary layer there may also be a higher inversion which is a fossil remnant of the highest level reached by a previous day's convection. Any disturbance of an inversion can cause waves to propagate on the stable layer.

The waves can be triggered by external flows such as the intrusion of a density current front, the descent of a shaft of cold air from a thunderstorm or the ascent of a thermal plume when vigorous convection is occurring. They can also be triggered by natural flows in the boundary layer.

5.4.4 Solitary Waves

Christie et al (1978) have described how a general disturbance will, over time, evolve into a series of solitary waves. (See Figure 18.) These solitary waves can then maintain their form as they propagate over large distances. In view of their long persistence, it is necessary to determine whether any of these solitary waves induce strong enough vertical currents to cause overload of an aircraft.

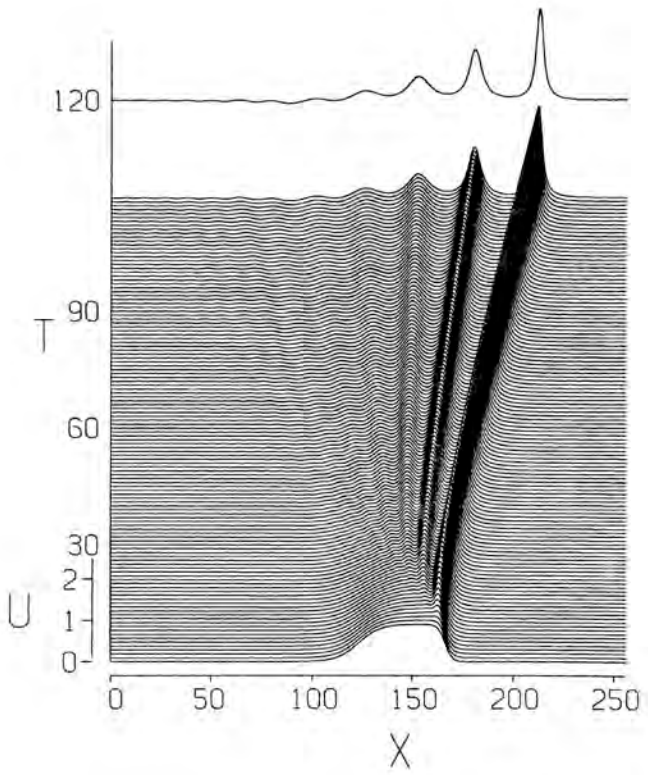

Figure 18: Evolution of an arbitrary wave form into a sequence of solitons [After Christie & Muirhead (1983a)]

Christie et al have observed solitary waves using an array of sensitive pressure sensors located at Warramunga, near Tennant Creek in the arid interior of the Northern Territory of Australia. The flow inside a solitary wave is thought to be a vortex, which is sometimes made evident as a roll cloud. The Morning Glory is one example, but not the only one. See, for example, Robin (1978). Christie et al observed 99 events over a two year period. Pressure waves had amplitudes up to 1.1 hPa. They propagate with speeds between 4 and 18 m/s and have a full width at half maximum amplitude of between 0.4 and 7.7 km.

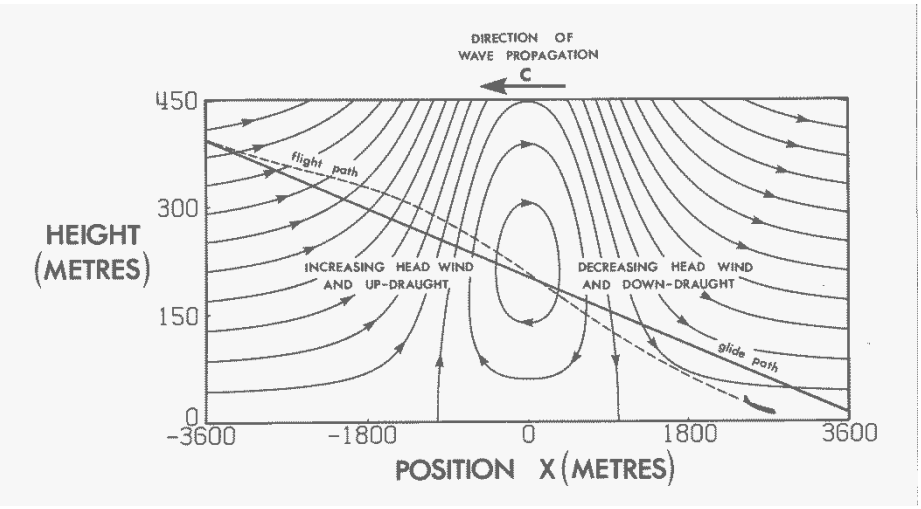

Figure 19: Streamlines in a solitary wave [after Christie & Muirhead (1983b)]

Christie and Muirhead (1983a) examined the flow within a solitary wave and determined that the updraft and downdraft were typically 5 m/s but could easily exceed 8 m/s. Figure 19 shows a theoretical picture of a solitary wave. The width of the steep gradient portion of this updraft or downdraft is typically 900 m, which is rather longer than the gust wavelength to cause maximum aircraft response. So the long gust gradient distance, combined with the 8 m/s common maximum gust suggests that the vertical gusts caused by a solitary wave will not cause a structural overload[26].

However, actual measurements indicate that shorter gust gradient distances may be involved. Cheung and Little (1990) have separately measured the passage of five solitary waves over a 300 m instrumented tower. They observed a maximum change in vertical velocity at the 200 m level, with a change of about 4 m/s in 8 seconds and a horizontal wind speed of almost 7 m/s. This corresponds to a gust gradient distance of 56 m, which is in the range of most concern to an aircraft, but the change of 4 m/s was much less than a limit load value. On the other hand, the sample of five events was too small to have confidence that a limit load would not be encountered.

A further measurement has been reported by Sun et al (2004), but again, the maximum change in vertical velocity was only about 3 m/s.

A notable example of a solitary wave train is the Morning Glory of the Gulf of Carpentaria. This is seen at sunrise as "a long horizontal roll cloud which appears on the eastern skyline, usually in calm and cloudless conditions and advances rapidly, like a rolling sea wave, bringing with it a sudden wind squall but rarely any precipitation" (Neal et al. 1977). It appears to be triggered when a sea breeze from the East side of the Cape York peninsula interacts with a stable layer formed during the night on the west side of the peninsula. Clarke et al (1981) reported the results of an expedition in 1979 to measure characteristics of several Morning Glories. Their program included multiple aircraft

[26] This does not negate the possibility, suggested in Figure 19, that the longitudinal shear of the vertical wind component may cause a control problem for the aircraft.

penetrations of each of two Morning Glories. The instrumentation was rudimentary with vertical velocities inferred by orally reading airspeed, altitude and rate of climb onto a tape recorder at approximately 10 second intervals. These measurements were supplemented by 2-theodolite measurements of pilot balloons released at 5 – 10 minute intervals around the time of passage of each Morning Glory. Vertical velocities changed from +4 m/s to -4 m/s in a distance of around 2 km. These magnitudes are probably not of concern, even though they involve a lot of averaging and the worst case is probably sharper than is indicated by the crude measurements.

Question 7: Is there a larger set of measurements of vertical wind speed during the passage of solitary waves, or, indeed, of the more irregularly shaped waves that occur where the disturbance originates?

5.4.5 Breaking Waves

Steady waves may transport energy a long distance with very little energy loss. The flow pattern in the wave may be fairly simple. It may also be of too long a wavelength to produce maximum aircraft response. A breaking wave introduces perturbations on this flow that may result in a more significant gust to an aircraft. Further work is required to evaluate whether this is the case. The effects of breaking waves in the atmosphere have been considered by Bretherton (1969), Fritts (1989) and Lott (2003 appr.)

Figure 20 is taken from Ellis (1978). It shows an aircraft turbulence encounter that looks as if it might be a breaking wave. This event occurred at 10,000 ft, which could have been at the top of the boundary layer in a hot climate region, but it might also have been in a mountain wave. The geographic location of this incident cannot be determined from the limited information given by Ellis. However, the characteristics of a breaking wave are the same, no matter whether this was at the top of the ABL or not. The centre of gravity normal acceleration trace shows a fall-off, followed by a linear rise, and finishes with another fall off. This could be a steady wave pattern. But added to the general trend are some large oscillations at around 0.5 – 1 Hz. Both the steady wave and the breaking wave may cause significant vertical gusts.

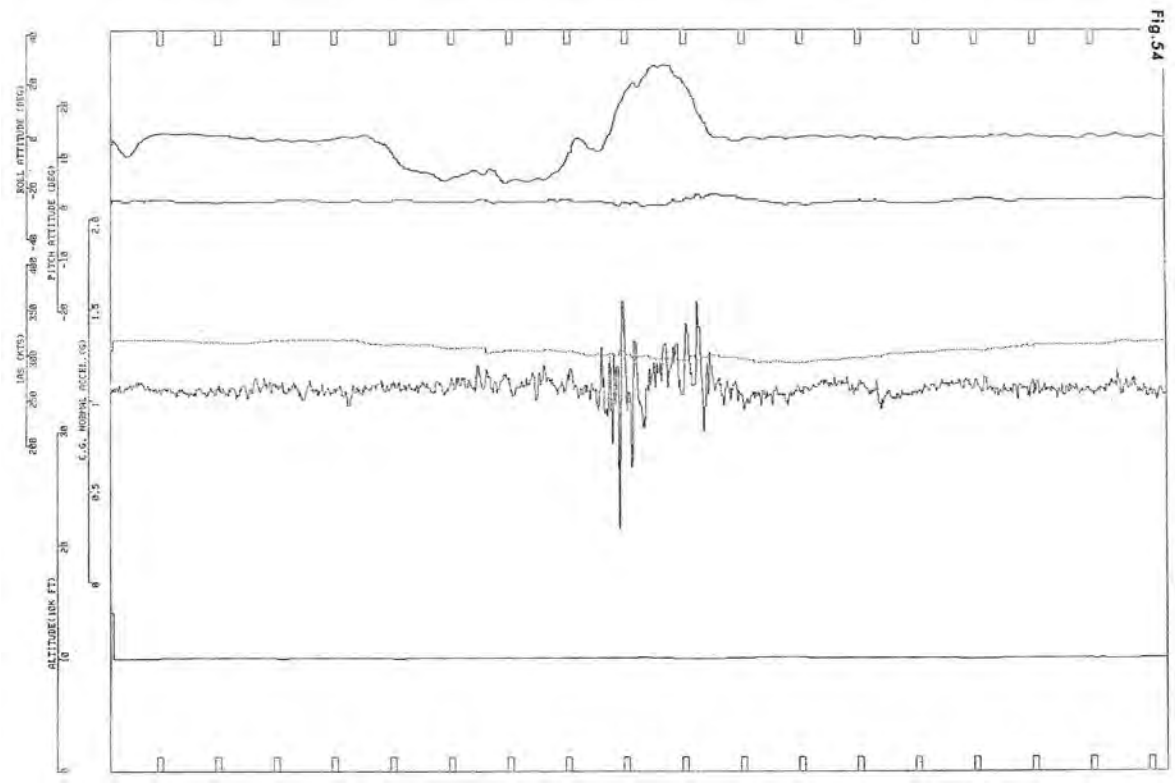

Figure 20: Example of a Turbulence Encounter, possibly with a breaking wave. From the top, the graphs show roll angle, pitch angle, indicated air speed, normal acceleration and altitude. The time marks (top and bottom of frame) are at 10 second intervals. (After Ellis (1978))]

Perhaps the pictures of breaking ocean waves that are shown in Clark Little's gallery, http://www.clarklittlephotography.com/gallery/ will give some insight into the sort of flow pattern that can occur. But because the density difference is so much less in the stratified atmosphere, the scale of the waves is of the order of 1000 times larger than water waves

5.5 Secondary Flows: Mesoscale Shallow Convection

Turbulence is generally a fine scale process. According to Sorbjan[27] (1989) turbulent flow as a whole may become unstable and lead to the initialisation of secondary motions. One form of secondary flow is a set of roll vortices whose axes are usually aligned approximately in the direction of the mean flow. Another is in the form of a set of hexagonal cells called mesoscale cellular convection.

Rolls are often evidenced by parallel lines of cloud streets that form in the regions of upward moving air. They have been reviewed by Etling and Brown (1993). The roll vortices are physically large. Vertical dimension is equal to the boundary layer thickness, whilst the lateral dimension is typically 2 to 10 times as large. The velocity of these vortices appears to be fairly small, but due to their large size, they have a large impact on the fluxes

[27] See Sorbjan page 34.

of heat, moisture and pollutants because they act to concentrate development of convective plumes into lines. Typical vertical velocities in rolls are usually less than 1 m/s (Stull 1988), but by sweeping convective thermals into lines, retardation of the ascending plumes by entrainment is reduced (the flow tends more towards two dimensional), so this may enhance updrafts along the cloud street lines. Rolls, with their attendant cloud streets, may be observed over land or sea, but are usually seen most clearly when cold air flows over a relatively warm ocean, probably because the uniform ocean surface lacks the irregular albedo that may lock terrestrial heat sources to terrain features.

Mesoscale cellular convection appears to occur in similar situations. Stull (1988) indicates that, over the ocean, roll patterns, with their attendant cloud streets, gradually change into hexagonal cellular patterns further downstream in a cold air advection situation. These cells have horizontal dimensions in the range 10 to 100 km, and depths around 2 to 3 km. There are two forms of cellular convection: one with updrafts at the cell boundaries and downdraft over the centre of the cell and one with the flow in the reverse direction (Atkinson and Zhang 1996).

Question 8: Is the magnitude of vertical velocities in secondary flows always small compared to aircraft design gusts of, say, 15 m/s?

6. Conclusion

This report has reviewed most, if not all, possible mechanisms that may cause gusts in the lowest 5,000 ft of the atmosphere. It tentatively concludes that there are only two, or possibly three, mechanisms that may cause gusts with sufficient magnitude to cause failure of an aircraft structure.

To determine probabilities of extreme loads requires a very large database. This report has examined some new gust statistics, documented by de Jonge et al (1994), for the design and certification of aircraft. It has been hypothesised that the new statistics are much too severe in the lowest part of the atmosphere. However, this hypothesis can only be supported if there is no cause of extreme vertical gusts in the lowest 5,000 ft of the atmosphere other than thunderstorms, mountain waves and, perhaps, in rare dust devils.

The writer is seeking a peer review by research and aviation meteorologists into whether this hypothesis can be supported. To assist consideration of this hypothesis the report has reviewed possible causes of vertical gusts in the lower layer of the atmosphere. None of the phenomena discussed here appear to be severe enough to cause a limit load on an aircraft. But in most cases, the writer has not been able to discover sufficient data to be sure of this.

Are there physical arguments, such as those advanced by Renno for vertical gusts in strong convecton (see Appendix A), which could be used to determine an upper bound on the vertical velocities induced by any of these phenomena? Are there larger databases of vertical velocities measured in various phenomena? Are there other phenomena that should be considered?

Readers are invited to communicate with the author[28] if they are interested or can make any contribution to the issues discussed or advance any of the questions raised above and collected below.

7. Aggregation of Questions

In pursuit of the main question of whether low altitude vertical gust magnitudes, outside thunderstorms and mountain waves, are bounded by a lesser value than would cause structural failure of an aircraft, the following questions have been formulated:

Question 1: Is there any effect of terrain on mountain waves that would make the probability of associated vertical gusts at low altitude significantly greater than would be predicted by extrapolation from higher altitudes?

Question 2: What is known about the rate of change of vertical velocity with radial distance at the side of a plume? What is the range of thickness of the shear layer at the side of a plume?

Question 3: Further consideration needs to be given to the generation of "dust devils" when the cause of the intense updrafts is a cold air outflow over a relatively warm surface. Are there any factors acting (e.g. suddenness of the cold flow) that might make the problem different from the archetypal gradually increasing heat over a desert.

Question 4: What is the mechanism and quantitative analysis for generation of vertical axis vortices at the leading edge of a cold front?

Question 5: Is there data on the maximum vertical gusts occurring in conjunction with dry cold fronts and with moist cold fronts that do not develop into thunderstorms?

Question 6: Are there any histograms of temperature drops behind sea breezes, cold fronts and haboobs? Are there any other forms of density currents that should be considered?

Question 7: Is there a larger set of measurements of vertical wind speed during the passage of solitary waves, or, indeed, of the more irregularly shaped waves that occur where the disturbance originates?

Question 8: Is the magnitude of vertical velocities in secondary flows always small compared to aircraft design gusts of, say, 15 m/s?

[28] Douglas.Sherman@dsto.defence.gov.au or stormboy70@outlook.com. Readers who wish to follow this subject are invited to email their contact details, as the writer intends to develop some type of discussion group so that contributions are visible to everyone.

8. Acknowledgement

The writer thanks Jorg Hacker, Mark Hibberd, Bruno Neininger, John Rustenburg and Alastair Williams for reviewing and making useful suggestions on an earlier draft of this document, and Katharine Kanak for comments on a preliminary version of Appendix A: .

9. References

Note: The Australian Meteorological Magazine (AMM) and its successor, The Australian Meteorological and Oceanographic Journal (AMOJ), are published by the Australian Bureau of Meteorology. Articles in these journals are indexed and may be retrieved at http://www.bom.gov.au/amm/ by clicking on "Papers".

Ansmann, A., M. Tesche, P. Knippertz, E. Bierwirth, D. Althausen, D. Műller and O. Schulz (2009). Vertical profiling of convective dust plumes in southern Morocco during SAMUM. Tellus B **61**(1): 340-353.

Arritt, R. W. (1993). Effects of the large-scale flow on characteristic features of the sea breeze. Journal of Applied Meteorology **32**: 116-125.

Atkinson, B. and J. W. Zhang (1996). Mesoscale shallow convection in the atmosphere. Reviews of Geophysics **34**(4): 403-431.

Bell, F. (1967). Dust devils and aviation. Bureau of Meteorology Australia. **Meteorological Note 27**.

Bretherton, F. (1969). Waves and turbulence in stably stratified fluids. Radio Science **4**(12): 1279-1287.

Brown, G. and J. Lopez (1990). Axisymmetric vortex breakdown Part 2. Physical mechanisms. Journal of Fluid Mechanics **221**(1): 553-576.

Cantor, B. A., K. M. Kanak and K. S. Edgett (2006). Mars Orbiter Camera observations of Martian dust devils and their tracks (September 1997 to January 2006) and evaluation of theoretical vortex models. Journal of geophysical research **111**(E12): E12002.

Charba, J. (1974). Application of gravity current model to analysis of squall-line gust front. Mon. Wea. Rev. **102**: 140-156.

Cheung, T. K. and C. G. Little (1990). Meteorological tower, microbarograph array, and sodar observations of solitary-like waves in the nocturnal boundary layer. Journal of Atmospheric Sciences **47**: 2516-2536.

Christie, D. R. and K. J. Muirhead (1983a). Solitary waves- A low-level wind shear hazard to aviation. International Journal of Aviation Safety **1**: 169-190.

Christie, D. R. and K. J. Muirhead (1983b). Solitary waves: A hazard to aircraft operating at low altitudes. Aust. Met. Mag. 31(1983) pp.97-109.

Christie, D. R., K. J. Muirhead and A. L. Hales (1978). On solitary waves in the atmosphere. Journal of the Atmospheric Sciences **35**(5): 805-825.

Clarke, R. (1983). Fair weather nocturnal inland wind surges and atmospheric bores: Part I Nocturnal wind surges. Aust. Met. Mag **31**: 133-145.

Clarke, R., R. Smith and D. Reid (1981). The morning glory of the Gulf of Carpentaria: an atmospheric undular bore. Monthly Weather Review **109**(8): 1726-1750.

Conangla, L. and J. Cuxart (2006). On the turbulence in the upper part of the low-level jet: an experimental and numerical study. Boundary-Layer Meteorology **118**(2): 379-400.

Cowled, L. H. (1988). An Aircraft Encounter wiht Severe Low Level Cold Frontal Turbulence. Master of Science, Monash University.

de Jonge, J. B. (1994). Reduction of Incremental Load Factor Acceleration Data to Gust Statistics, National Aerospace Laboratory, The Netherlands. **DOT/FAA/CT-94/57**.

de Jonge, J. B., P. A. Hol and P. A. v. Gelder (1994). Reanalysis of European Flight Loads Data. U.S. Department of Transport. **DOT/FAA/CT-94/21**.

Defant, A. (1921). Ueber die Dynamik der Boen: Beitr. Phys. Frei Atmos **9**: 99-113.

Dutton, J. A., G. J. Thompson and D. G. Deaven (1968). The Probabilistic Structure of Clear Air Turbulence—Some Observational Results and Implications. Clear Air Turbulence and its Detection. Y.-H. Pao and A. Goldburg. New York, Plenum Press**:** 183-206.

Eissa, Y., P. R. Marpu, I. Gherboudj, H. Ghedira, T. B. M. J. Ouarda and M. Chiesa (2013). Artificial neural network based model for retrieval of the direct normal, diffuse horizontal and global horizontal irradiances using SEVIRI images. Solar Energy **89** 1-16.

Ellis, S. D. (1978). A Presentation of Measured Aircraft Responses in Turbulence During Civil Operations. Technical Report. Farnborough, Hants, Royal Aircraft Establishment,. **RAE-TR-78113:** 106 pp.

Etling, D. and R. Brown (1993). Roll vortices in the planetary boundary layer: A review. Boundary-Layer Meteorology **65**(3): 215-248.

Fairall, C., A. White, J. Edson and J. Hare (1997). Integrated shipboard measurements of the marine boundary layer. Journal of Atmospheric and Oceanic Technology **14**(3): 338-359.

Federal Aviation Administration (1980). Federal Aviation Regulations Part 25: Airworthiness Standards: Transport Category Airplanes.

Finkele, K., J. M. Hacker, H. Kraus and R. A. D. Byron-Scott (1995). A complete sea-breeze circulation cell derived from aircraft observations. Boundary-Layer Meteorology **73**(3): 299-317.

Fritts, D. C. (1989). A review of gravity wave saturation processes, effects, and variability in the middle atmosphere. Middle Atmosphere, Springer**:** 343-371.

Fujita, T. T. (1986). DFW Microburst on August 2, 1985 University of Chicago,.

Garrison, J. N. (1971). An assessment of atmospheric turbulence data for aeronautical applications. Conference on Atmospheric turbulence 18-21 May. London, Royal Aeronautical Society

Grace, W. and I. Holton (1990). Hydraulic jump signatures associated with Adelaide downslope winds. Aust. Met. Mag **38**: 43-52.

Graf, A., D. Schüttemeyer, H. Geiß, A. Knaps, M. Möllmann-Coers, J. H. Schween, S. Kollet, B. Neininger, M. Herbst and H. Vereecken (2010). Boundedness of turbulent temperature probability distributions, and their relation to the vertical profile in the convective boundary layer. Boundary-Layer Meteorology **134**(3): 459-486.

Hess, G. and K. Spillane (1990). Characteristics of dust devils in Australia. Journal of Applied Meteorology **29**: 498-507.

Hess, G. D. and K. T. Spillane (1988). Estimation of the parameters of convection dynamics. Journal of Aircraft **25**: 862-864.

Hess, G. D., K. T. Spillane and R. S. Lourensz (1988). Atmospheric Vortices in Shallow Convection. Journal of Applied Meteorology **27**(3): 305-317.

Hoblit, F. M., N. Paul, J. D. Shelton and F. E. Ashford (1966). Development of a power spectral gust design procedure for civil aircraft. Technical Report. FAA, Federal Aviation Agency. **FAA-ADS-53**.

Hull, D. (1994). Design limit loads based upon statistical discrete gust methodology. Aircraft Loads due to Turbulence and their Impact on Design and Certification, Lillehammer, Norway.

Idso, S. B. (1976). Dust storms. Scientific American **235**(4).

Ives, R. L. (1947). Behavior of dust devils. Bull. Amer. Meteor. Soc **28**: 168-174.

Jones, J. G. (2004). "Documentation of the Linear Statistical Discrete Gust Method." DOT/FAA/AR-04/20, from http://www.tc.faa.gov/its/worldpac/techrpt/ar04-20.pdf.

Kaimal, J. and J. Businger (1970). Case studies of a convective plume and a dust devil. Journal of Applied Meteorology **9**: 612-620.

Kaimal, J., J. Wyngaard, D. Haugen, O. Coté, Y. Izumi, S. Caughey and C. Readings (1976). Turbulence structure in the convective boundary layer. Journal of the Atmospheric Sciences **33**(11): 2152-2169.

Kolmogorov, A. N. (1941). Dissipation of energy in locally isotropic turbulence. Doklady Akademii Nauk SSSR **32**(1): 16-18.

Kraus, H., C. Ewenz, M. Kremer and J. Hacker (2000). The multi-scale structure of the Australian cool changes. Meteorology and Atmospheric Physics **73**(3-4): 157-175.

Lopez, J. (1990). Axisymmetric vortex breakdown Part 1. Confined swirling flow. Journal of Fluid Mechanics **221**(1): 533-552.

Lott, F. (2003 appr.). "Large-Scale Flow Response to the Breaking of Mountain Gravity Waves." from http://www.lmd.jussieu.fr/~flott/seminaire/NIO_v1.pdf.

McCaul Jr, E. W., H. B. Bluestein and R. J. Doviak (1986). Airborne Doppler lidar techniques for observing severe thunderstorms. Applied optics **25**(5): 698-708.

Membery, D. A. (1985). A Gravity-Wave Haboob? Weather **40**(7): 214-221.

Mueller, C. K. and R. E. Carbone (1987). Dynamics of a thunderstorm outflow. Journal of the Atmospheric Sciences **44**(15): 1879-1898.

Neal, A. B., I. J. Butterworth and K. M. Murphy (1977). The morning glory. Weather, 32:176-183.

Neuls, G. S., H. G. Maier, T. R. Lerwick, E. A. Robb and I. J. Webster (1962). Optimum fatigue spectra, second phase report. USAF Aeronautical Systems Division. **ASD-TR-61-235**.

Poulos, G. S., W. Blumen, D. C. Fritts, J. K. Lundquist, J. Sun, S. P. Burns, C. Nappo, R. Banta, R. Newsom and J. Cuxart (2002). CASES-99: A comprehensive investigation of the stable nocturnal boundary layer. Bulletin of the American Meteorological Society **83**(4): 555-581.

Press, H. and R. Steiner (1958). An approach to the problem of estimating severe and repeated gust loads for missile operations. NACA Technical Note. **4332**.

Reeder, M. J. and R. K. Smith (1992). Australian spring and summer cold fronts. Aust. Met. Mag **41**: 101-124.

Rennó, N. O., M. L. Burkett and M. P. Larkin (1998). A simple thermodynamical theory for dust devils. Journal of the Atmospheric Sciences **55**(21): 3244-3252.

Rennó, N. O. and A. P. Ingersoll (1996). Natural convection as a heat engine: A theory for CAPE. Journal of the Atmospheric Sciences **53**(4): 572-585.

Roach, W. and J. Findlater (1983). An aircraft encounter with a tornado. Meteor. Mag **112**: 29-49.

Robin, A. (1978). Roll cloud over Spencer Gulf. Aust. Met. Mag **26**: 125.

Ryan, J. A. and J. J. Carroll (1970). Dust Devil Wind Velocities: Mature State. J. Geophys. Res. **75**(3): 531-541.

Sherman, D. J. (2013). Gust clearance of RAAF C-130J-30 Hercules aircraft. DSTO Technical Report. **Unpublished Report**.

Simpson, J. (1969). A comparison between laboratory and atmospheric density currents. Quarterly Journal of the Royal Meteorological Society **95**(406): 758-765.

Simpson, J., D. Mansfield and J. Milford (1977). Inland Penetration of Sea-Breeze Fronts. Quarterly Journal of the Royal Meteorological Society **103**: 47-76.

Sinclair, P. C. (1966). A Quantitative Analysis of the Dust Devil. Ph D, University of Arizona.

Sorbjan, Z. (1989). Structure of the atmospheric boundary layer, Prentice Hall

Stewart, R. H. (2005). "Introduction to Physical Oceanography: Chapter 5 - The Oceanic Heat Budget - Geographic Distribution of Terms in the Heat Budget." from http://oceanworld.tamu.edu/resources/ocng_textbook/chapter05/chapter05_06.htm.

Stull, R. B. (1988). An introduction to boundary layer meteorology, Springer.

Sun, J., D. H. Lenschow, S. P. Burns, R. M. Banta, R. K. Newsom, R. Coulter, S. Frasier, T. Ince, C. Nappo and B. B. Balsley (2004). Atmospheric disturbances that generate intermittent turbulence in nocturnal boundary layers. Boundary-Layer Meteorology **110**(2): 255-279.

Tjernström, M., B. B. Balsley, G. Svensson and C. J. Nappo (2009). The Effects of Critical Layers on Residual Layer Turbulence. Journal of the Atmospheric Sciences **66**(2): 468-480.

Tyrell, J. D. (1999). An airborne encounter with a whirlwind over County Kerry, Ireland. Journal of Meteorology (Trowbridge then Bradford on Avon) **24**(244): 404-410.

Ulden, A. P. and J. Wieringa (1996). Atmospheric boundary layer research at Cabauw. Boundary-Layer Meteorology **78**(1): 39-69.

Webb, E. (1984). Temperature and humidity structure in the lower atmosphere. Geodetic Refraction, Springer**:** 85-141.

Webb, E. K. (1977). Convection mechanisms of atmospheric heat transfer from surface to global scales. Second Australasian Conference on Heat and Mass Transfer. University of Sydney, CSIRO, Aspendale (Australia). Div. of Atmospheric Physics.**:** 523-239.

Weller, R. and S. Anderson (1996). Surface meteorology and air-sea fluxes in the western equatorial Pacific warm pool during the TOGA Coupled Ocean-Atmosphere Response Experiment. Journal of Climate **9**(8): 1959-1990.

Williams, A. and J. Hacker (1992). The composite shape and structure of coherent eddies in the convective boundary layer. Boundary-Layer Meteorology **61**(3): 213-245.

Williams, A. and J. Hacker (1993). Interactions between coherent eddies in the lower convective boundary layer. Boundary-Layer Meteorology **64**(1-2): 55-74.

Wilson, J. W. (1986). Tornadogenesis by nonprecipitation induced wind shear lines. Monthly Weather Review **114**(2): 270-284.

Wingrove, R. C. and R. Bach (1994). Severe turbulence and maneuvering from airline flight records. Journal of Aircraft **31**(4): 753-760.

Wood, R., I. Stromberg and P. Jonas (1999). Aircraft observations of sea-breeze frontal structure. Quarterly Journal of the Royal Meteorological Society **125**(558): 1959-1995.

Wyngaard, J. C. (2010). Turbulence in the Atmosphere. Cambridge, Cambridge University Press.

Appendix A: Conversion of Heat Energy to Mechanical Energy

A.1. The Heat Engine Model

The atmosphere functions as a heat engine so, as with any heat engine, only a fraction of the heat energy input can be converted to mechanical energy. The fraction that can be converted depends on the temperatures at which heat is input and rejected.

A heat engine must have a heat source and a heat sink. The heat source comes as the sun warms the ground and the hot ground, in turn, supplies heat to the air near ground level. When the ground is moist, the main part of the energy input is in the form of latent heat carried as water vapour. When the ground is dry, the main part of the heat input is as sensible heat. As the heated air rises, a fraction of the energy is converted into kinetic energy of motion and part of this is the rising gust whose magnitude is desired. Eventually these gusts turn into turbulence which is dissipated as heat at high altitudes. The heat sink of this engine is where the descending air outside the plume radiates its heat back to its surroundings and the sky.

The greatest possible efficiency of a heat engine is η, which is given by:

$$\eta = \frac{T_H - T_C}{T_H}$$

where T_H is the absolute temperature of the heat source and T_C is the absolute temperature of the heat sink. η is the maximum fraction of the input heat energy that can be converted to mechanical energy.

On this basis, Renno and Ingersoll (1996) developed an equation for the maximum vertical velocity in a plume or vortex in the form:

$$w = \left[\left(\frac{c_p}{8\varepsilon\sigma_R T_c^3}\right)\frac{\eta F_{in}}{\mu}\right]^{1/2}$$

The meaning of the various symbols and the typical values used for convective plumes [Renno and Ingersoll (1996)] and for dust devils [Renno et al (1998)] are shown in Table 3.

Table 3: Typical values used by Renno in modelling deep convection and dust devils

Symbol	Meaning	Units	Value Renno & Ingersoll 1996 Deep Convection	Value Renno et al 1998 Dust Devil
c_p	Specific heat at constant pressure	J Kg^{-1} K^{-1}	1005	1005
ε	Emissivity of air "slab"		0.7	0.7
σ_R	Stefan Boltzmann constant	W m^{-2} K^{-4}	5.67E-8	5.67E-8
T_H	Temperature of heat source	K	299	316
T_C	Temperature of heat sink	K	269	298
η	Thermodynamic efficiency		0.1	0.05
F_{in}	Input heat flux	W m^{-2}	155	455
μ	Mechanical energy dissipation coefficient		16	10 – 50
w	Convective velocity	m s^{-1}	12	8 – 16

To find extreme values, it is necessary to examine some of the parameters in Renno's equation, especially the temperatures of the heat source and sink and the input energy intensity.

In intense atmospheric convection there is a very high, super-adiabatic, temperature gradient adjacent to the ground. The temperature gradient decreases with increasing distance above the ground until it reaches the adiabatic lapse rate. Temperature traces measured by Sinclair (1966) near Tucson, Arizona show temperatures at 7 ft above ground are typically 3 to 5 degrees warmer than those at a height of 17 ft, whilst temperatures at 17 ft are very similar to those at 31 ft. [See Figure 2 of Renno et al (1998) which is reproduced from Sinclair's thesis.] With a smooth ground surface, there may be a "micro-layer" of air adjacent to the ground, of the order of 1 cm thick, where heat transfer is entirely by molecular conduction. Air is a poor conductor, so the temperature gradient is very high. In progressively thicker layers above the conduction layer, the temperature gradient gradually diminishes towards the adiabatic value. It might be conjectured that convection is occurring in the near ground layers, but the size of convection cells near the ground is limited to something comparable to the distance above ground. Thus the scale of convective cells increases with increasing distance from the wall, so the resistance to heat transfer gradually decreases. The first layer against the wall only involves molecular transfer, so the air in that layer does not convect. Therefore, the source temperature for the convection should be the temperature at the top of this layer. The temperature gradient in the micro-layer is very large and it is difficult to determine the thickness of the micro-layer; hence it is difficult to determine accurately the temperature of the heat source.

The heat sink is the air in the convective layer outside the ascending column. For deep convection (thunderstorms), the convective layer may be the whole troposphere ("deep convection") and for dry convection, including dust devils, it may be confined within the ABL. Most of the heat loss is assumed to occur in the slowly descending air surrounding

the plume or dust devil. Renno & Ingersoll (1996) take the heat sink temperature as the "entropy weighted mean temperature of the layer emitting infra-red radiation". In the case of deep convection, the air in the rising plume is quite hot for its altitude, because of the latent heat released by condensation of the rising moist air. Renno & Ingersoll assume that, since the air around the plume descends very slowly, the air loses heat as it descends, so its temperature at any level is comparable to the surrounding environment. Renno argues that, approximately, the temperature of the heat sink is the mean temperature in the atmospheric layer outside the rising column.

A.2. Extreme values

Renno's assumed parameter values, shown in Table 3 are typical values for strong convection but an attempt will now be made to use Renno's equation to predict extreme values of the vertical convective velocity.

A.2.1 Extreme Insolation

The input energy comes from the sun's radiation. The solar irradiance outside the atmosphere is 1380 W m^{-2} but not all of this reaches the ground. Stewart (2005) indicates the average balance of radiant energy between sun, earth and atmosphere. The total amount of radiation, from all sources, received at the earth's surface is called the Global Horizontal Irradiance (GHI). This varies significantly with time of day, latitude and the condition of the atmosphere. Eissa et al (2013) show graphs of measured GHI in Saudi Arabia, which can probably be considered to be as severe as anywhere in the world. The maximum daily value occurs near midday and typical values from their paper are shown in Table 4. Only a part of this energy is available to warm the air in the convective layer. Some of the heat is absorbed by the soil. The rest must pass through the micro-layer by conduction before it can be used to drive convection. The result is that worst case values of F_{in} are usually limited to about 500 W m^{-2} and possibly rising to 750 W m^{-2} for an extreme case, occurring with very severe dry convection in a desert environment.

Table 4: Typical maximum daily values of Global Horizontal Irradiance (GHI) in Saudi Arabia (after Eissa et al)

Sky Condition	GHI (W m^{-2})
Heavy dusty day	700
Moderate dusty day	900
Clear day	1000

When moist convection is occurring, part of the sky is obscured by clouds, whilst moisture in the ground reduces both the heat source temperature and the flux of input energy. In these conditions, most of the input energy can be in the form of latent heat rather than sensible heat. This explains the relatively low value of 155 W m^{-2} used by Renno & Ingersoll (1996). The highest fluxes of latent heat are likely to occur over the warm oceans. Weller and Anderson (1996) have shown variations of heat fluxes measured during the TOGA-COARE, at the warm pool that covers a large part of the Tropical West Pacific

where average rainfall and latent heat release have global maxima. In that experiment, the greatest spike in the latent heat flux was approximately 400 W m^{-2}.

A.2.2 Extreme Hot and Cold Reservoir Temperatures

The temperature of the heat sink is a key item in calculating the efficiency of the heat engine. Renno suggests the entropy weighted temperature in the descending air outside the downdraft, and then approximates this by the mean of the temperature at the surface and the temperature in the ambient atmosphere at the level of the top of the convective process.

For dry convection, consider the atmospheric sounding shown in Figure 28 of Cantor et al (2006) which was measured in the late afternoon of a day on which dust devil activity was occurring. The temperature trace follows the dry adiabat very closely up to about the 540 mb level. This sounding is especially representative because it was taken late in the day, after most convective mixing had taken effect and before night time cooling had set in. This gives us justification to assume a dry adiabatic temperature profile over most of the convective layer, with the super-adiabatic gradient being mostly confined to the very low levels. [Note, however, that Ives (1947) measured twice the adiabatic lapse rate between 5 ft and 2000 ft altitude. This may be due to different techniques he used between ground based and aircraft based measurements, or it may be due to a much thicker super-adiabatic layer over very hot desert.] To get an extreme case, consider the Moroccan observations described by Ansmann et al (2009). Some plumes were observed to be greater than 2 km in height, and the dust layer extended up to 4 km. On the 19 May, 2006, the ground surface temperature was observed to reach 58°C and the air temperature at 2 m was 34°C. Assuming an adiabatic lapse rate from the 2 m altitude to 4 km would suggest a cold temperature of -6°C at 4 km altitude, with a cold sink temperature of 14°C (the mean of temperatures at 2 m and 4 km). The hot source temperature might be taken as 46°C. (This is half way between the ground temperature and the temperature at 2 m.)

In the case of moist convection, a parcel of rising air will follow a dry adiabat until the air becomes saturated, when it will follow a moist adiabat, which has higher temperatures than a dry adiabat at the same altitude due to heat released by condensing moisture. All the time the parcel is following the moist adiabat, moisture is condensing and thus forming cloud.

Figure 21 and Figure 22 show aerological diagrams for temperature soundings measured by meteorological balloons at Darwin on days when severe storm warnings were issued.

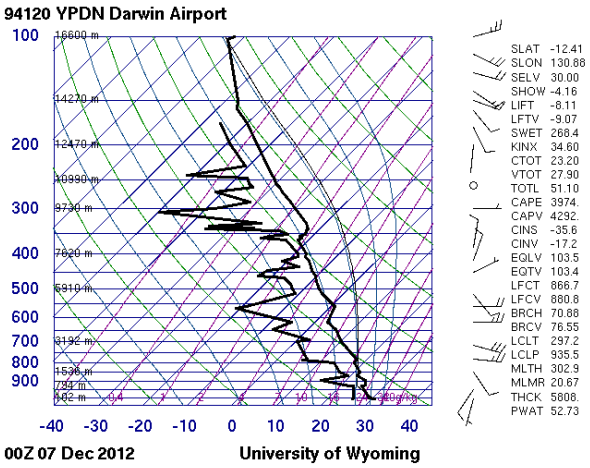

Figure 21: Aerological sounding at Darwin for 10 am local time, 7 December 2012[29]

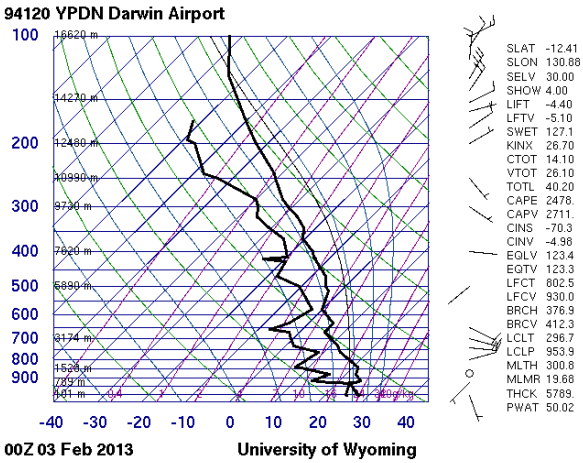

Figure 22: Aerological sounding at Darwin[30] *for 10 am local time, 3 February 2013.*

The two heavy black curves on each diagram show the measured dew point temperature (left hand curve) and dry bulb temperature (right hand curve). The thin black curve which, at mid-levels for these two cases, is well to the right (about 5° to 10°) of the dry bulb curve shows the temperature that would be taken by a parcel of air that rose from ground level. Where this temperature is greater than the measured dry bulb temperature, the parcel would be positively buoyant and would accelerate upwards. The area between this curve and the dry bulb trace is therefore a measure of the energy that would be available to cause severe moist convection. This area is called the Convective Available Potential Energy (CAPE) of the atmosphere. A value of 1000 J/kg is often exceeded on days when a thunderstorm occurs, whilst values of 5,000 J/kg occur in extreme situations. For these two curves, it will be seen from the numbers to the right of the two graphs that the CAPE is 3974 and 2478 respectively, justifying the severe storm warnings[31].

Once a parcel of surface air is lifted to a height where it is positively buoyant, it will continue moving upward until its temperature drops below that of the ambient air at the level. It may even overshoot somewhat before falling back to the equilibrium level. At this point the air spreads out, leaving the convective updraft and becoming part of the heat sink, as heat is lost by infra-red radiation[32] to the sky and surrounding air. Since the moist

[29] The University of Wyoming archives meteorological soundings from all around the world, hence its mention in the two diagrams.

[30] Darwin, in the wet season, will have a somewhat similar climate to the TOGA COARE area mentioned previously in connection with ascertaining an extreme value of latent heat flux into the atmosphere.

[31] Other factors, notably wind shear, are also involved in the likelihood of a severe storm.

[32] Infra-red covers the wavelengths from 0.74 μm to about 15 μm, with far infra-red extending to around 1000 μm. Kraus and Businger (1994), in chapter 3 of their textbook, indicate that most of the infra-red energy is radiated by the minor H_20, CO_2, O_3, N_2O and CH_4 components of the atmosphere.

convection necessitated condensation of moisture, the outspreading air will be visible as a canopy of upper level cloud.

Weather satellites photograph clouds in both visual and Infra-red wavelengths. The visual photographs show the reflected light from the sun whilst the infra-red imagery shows the infra-red intensity emitted directly by the target. In the infra-red imagery, strong radiances are shown dark and weak radiances as white. High altitude clouds are cold, emit little infra-red energy, so are shown as bright. The fact that the IR from below does not shine through indicates that the clouds are optically dense in the IR range used. The scanning is typically in the range 10.3-12.5 μm (IR4 and IR5 channels). The fact that the clouds are substantially opaque to these frequencies means most of the infra-red radiation from water molecules to space is coming from the top of the cloud. On this basis, the temperature of the cold sink should be biased towards the temperature of the air at the top of the cloud. The cold reservoir is, thus, colder than assumed by Renno.

On this basis, following the two aerological diagrams, one might take the cold temperature as -85°C. However, as the cloud canopy mixes with the dry air at altitude, some of the condensed moisture will re-evaporate. This re-evaporation will cool the air[33], but it will also remove the opacity surrounding the cloud top, enabling air at lower levels to also radiate heat to the sky. Thus, as a very crude assumption, one might take the cold sink temperature to be the one-third point between -85°C and the hot temperature of approximately +30°C at ground level. i.e. T_C=-47°C, T_H=30°C.

A.2.3 Extremes of Mechanical Energy Dissipation

The mechanical energy dissipation coefficient is the "wild and woolly" part of Renno's equation. Renno & Ingersoll (1996) use some hand waving arguments to derive μ~16, whilst in Renno et al (1998) the range is given as μ=10-50. Renno & Ingersoll (1996) call μ a "potentially tunable parameter of our scaling analysis". Here, their range of 10-50 will be used to, hopefully, bracket the predicted vertical velocity.

A.2.4 Extremes of Vertical Convection Velocity

Table 5 shows the computation of extreme values of convection velocity using Renno's equation and the extreme values of the various atmospheric parameters as discussed above. Following Renno, this table shows values for a low and a high value of the energy dissipation coefficient. This range should be viewed as a measure of the uncertainty in the computation rather than an indicator of the range of values that may physically occur. Since w varies inversely as the square root of μ, the larger value of w corresponds to the smaller value of μ.

[33] The absorbed heat will remain, as vapour, in the air, so remains part of the heat engine cycle. The resultant increase in density of the cooled air will cause the air to fall to a lower level.

Table 5: Extreme values used in modelling deep convection and dust devils using Renno's equation

Symbol	Meaning	Units	Value Deep Convection	Value Dust Devil
c_p	Specific heat at constant pressure	J Kg^{-1} °K^{-1}	1005	1005
ε	Emissivity of air "slab"		0.7	0.7
σ_R	Stefan Boltzmann constant	W m^{-2} °K^{-4}	5.67E-08	5.67E-08
T_H	Temperature of heat source	°K	303	319
T_C	Temperature of heat sink	°K	226	287
η	Thermodynamic efficiency		0.25	0.10
F_{in}	Input heat flux	W m^{-2}	400	750
μ	Mechanical energy dissipation coefficient		10 - 50	10 - 50
w	Convective velocity	m s^{-1}	24 - 53	14 - 32

Appendix B: A Note on Sea Breezes

At school it is taught that, during the day, the land heats up more than the sea. As a consequence the air above the land is also heated more than over the sea. The hot air rises, so the cooler air over the sea rushes in to replace it.

Simplistically, this gives rise to the thought that as the cold air flows on-shore, the upper level air will be displaced and flow out to sea, giving rise to a, so-called, "return flow".

Observations often note a horizontal temperature gradient near the coast, but the colder air does not commence to move inland until later in the day. Sometimes the expression is used that the sea breeze "sticks" until later in the day.

A real-life situation is complicated by such factors as pre-existing temperature profiles and synoptic winds. But to understand the elements of the flow, let us hypothesise no synoptic wind and an atmosphere that is horizontally homogeneous at the beginning of the day.

As the morning wears on, the air over the land will expand upwards more than the air over the sea. But this will not provide any driving force for the sea breeze to move inland, as, at sea level, the mass of air over each square metre of surface is the same over land as over the sea, so the pressure is the same. At a higher level, say 1 km, the air over the land has expanded upward more than over the sea, so there is more mass of air above a 1 square meter horizontal surface over land than over sea. Thus, at any altitude higher than the surface, the pressure is greater over land than over sea, so this will drive an off-shore flow at altitude. Once sufficient mass of air has moved off-shore, the pressure at sea level will become greater over the sea than over land and the sea breeze front will "unstick" and commence to move inland. Therefore, the off-shore flow at altitude is the primary flow: the sea breeze is actually the return flow.

The process of "unsticking" is actually quite complex. In the first place, as the convectively turbulent air in the layers above the surface layer moves off shore, it will exercise an off-shore drag, albeit small, on the cold air adjacent to the ocean. At the same time, in the first stages of the off-shore movement of air mass, the air will only have time to move a small distance. The extra pressure that results just off-shore, will exert a shore-ward force on a very small amount of the cold air adjacent to the coast, but it will also cause an off-shore pressure gradient on the air at the ocean surface further out to sea. Thus a very small amount of colder air may start to move inland, but the movement will be very slow, because the pressure gradient is only small and is only favourable for a very low depth of the colder air. As the day wears on, more air moves from over land to over the sea, and the extra mass is spread over a much greater distance off-shore. At this point, a greater thickness of cold air has a favourable pressure gradient, so a much thicker layer of air starts moving towards the land. Since the flow is thicker, it has a higher wave speed, so the front of the later moving air overtakes whatever air had started to move inland previously. However, during one day, the primary off-shore flow can only transport air mass for a limited distance. Beyond this distance, the pressure gradient on the cold air is still directed off-shore. Thus there is only a finite amount of cold air that can be pushed inland as a sea

breeze. This explains why a sea breeze only occurs as a pulse or cut-off circulation, (Simpson et al. 1977) not as a sustained flow.

DEFENCE SCIENCE AND TECHNOLOGY GROUP
DOCUMENT CONTROL DATA

1. DLM/CAVEAT (OF DOCUMENT)

2. TITLE

Extreme Vertical Gusts in the Atmospheric Boundary Layer

3. SECURITY CLASSIFICATION (FOR UNCLASSIFIED REPORTS THAT ARE LIMITED RELEASE USE (L) NEXT TO DOCUMENT CLASSIFICATION)

Document	(U)
Title	(U)
Abstract	(U)

4. AUTHOR(S)

Douglas J Sherman

5. CORPORATE AUTHOR

Defence Science and Technology Group
506 Lorimer St
Fishermans Bend Victoria 3207 Australia

6a. DST-Group NUMBER	6b. AR NUMBER	6c. TYPE OF REPORT	7. DOCUMENT DATE
DST-Group--TR-3160	AR-016-419	Technical Report	July 2015

8. FILE NUMBER	9. TASK NUMBER	10. TASK SPONSOR	11. NO. OF PAGES	12. NO. OF REFERENCES
2014/1130296/1	07/405	DGTA	47	76

13. DST Publications Repository

http://dspace.dsto.defence.gov.au/dspace/

14. RELEASE AUTHORITY

Chief, Aerospace Division

15. SECONDARY RELEASE STATEMENT OF THIS DOCUMENT

Approved for public release

OVERSEAS ENQUIRIES OUTSIDE STATED LIMITATIONS SHOULD BE REFERRED THROUGH DOCUMENT EXCHANGE, PO BOX 1500, EDINBURGH, SA 5111

16. DELIBERATE ANNOUNCEMENT

No Limitations

17. CITATION IN OTHER DOCUMENTS Yes

18. DST RESEARCH LIBRARY THESAURUS

Gusts, Turbulence, Aircraft Loads, Ultimate Load, Limit Load, Atmospheric Boundary Layer, Convection

19. ABSTRACT

Gust statistics proposed recently for the clearance of aircraft appear to be much too severe in the lowest 5,000 ft of the atmosphere. It is contended that extreme gusts in the lowest layers are only those caused by thunderstorms or mountain waves and that these are no more frequent in the lowest 5,000 ft than in the 5,000-10,000 ft layer, even although milder gusts may be more frequent. This document seeks a peer review of this contention. In order to guide formal discussion, a review of all causes of extreme gusts has been attempted so that the peer revie can address the various single issues involved.